Proceedings of an ESA-NASA Workshop on a

Joint Solid Earth Programme

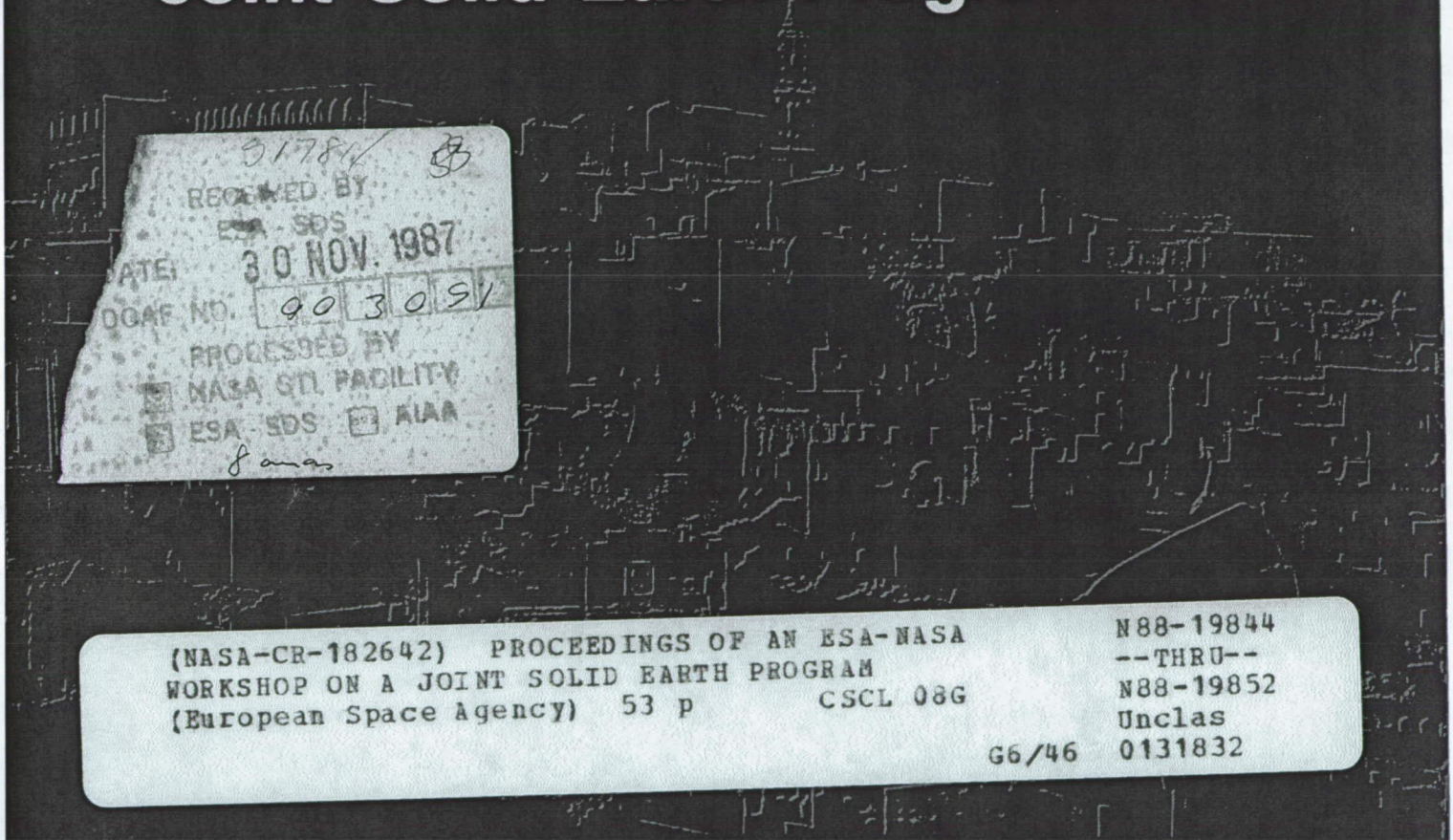

Matera, Italy
29-30 April 1987

Sponsored by:

The European Space Agency (ESA)
National Aeronautics & Space Administration (NASA)

esa
european space agency

esa SP-1094
October 1987
ISSN 0379-6566

Proceedings of an ESA-NASA Workshop on a

Joint Solid Earth Programme

Matera, Italy
29-30 April 1987

Sponsored by:

The European Space Agency (ESA)
National Aeronautics & Space Administration (NASA)

european space agency / agence spatiale européenne
8-10, rue Mario-Nikis, 75738 PARIS CEDEX 15, France

ESA SP-1094 — ISSN 0379-6566

ESA-NASA WORKSHOP ON A JOINT SOLID EARTH PROGRAMME

Matera, Italy, 29-30 April 1987

Proceedings published by: ESA Publications Division,
ESTEC, Noordwijk, The Netherlands

Edited by: T D Guyenne & J J Hunt

Printed in The Netherlands Price code: E2

Contents

KEYNOTE ADDRESS

P Goldsmith

Director of Earth Observation & Microgravity Programmes, ESA

Ladies and Gentlemen,

I welcome you to this Workshop. I am delighted to see so many participants today.

Many of you will remember the Workshop SESAME which was held one year ago, which set the guidelines on which we have been working during this past year. It is now realised that for a variety of reasons it is no longer possible to satisfy all the aspirations covered by SESAME recommendations in the foreseeable future.

However, we have not given up our efforts to promote a European space programme in Solid Earth, and today I can say that we have never been so close to an approved Solid Earth programme, since I believe this scientific community is close to agreeing its priorities. But I have to warn you that we will face a dead end if we cannot achieve a consensus on that one priority objective.

Let me first tell you where we stand today with our preparations for future Earth Observation Programmes in Europe: A revised Long-Term Space Plan is under preparation and will be submitted to an ESA Council meeting at ministerial level in November this year. It contains a broad scope of disciplines by a number of experimental and operational missions.

It is the front-end of this Programme which is of concern to your deliberations during this Workshop because the next two programme decisions in 1987 and 1988 are planned for:

- a second flight unit of the ERS-1 remote sensing satellite for a launch in 1993 (ERS-2)
- a Solid Earth Programme for a parallel (double) launch with ERS-2 in 1993.

ERS-2 has received recently 'seed money' for the procurement of long-lead items.

For a Solid Earth Programme I intend to submit to ESA Member States a first programme proposal within two months from now.

I also want to show them that the proposed programme meets the objectives of the large user community and that its development will be followed by an intensive and successful utilisation.

This is one reason why we convened this meeting today at rather short notice. The other reason is that the concept and its possible variations are identified to a degree where space industry can assess the technological challenge involved and can prepare themselves for a role in such a programme.

Another point is essential in this context:

The proposed Solid Earth Programme (or the European element of a joint development with the US) will be what we call an *optional* programme. This means that only those Member States which are interested in it will subscribe to it, and the amount of their funding share will reflect the degree to which they are convinced that they are investing into a worthwhile endeavour. Also they will wish to be convinced that the programme is planned in the most cost-effective way, hence the attractions of the shared launch with ERS-2 to the benefit of both programmes.

Proceedings of an ESA-NASA Workshop on a Joint Solid Earth Programme, Matera, Italy, 29-30 April, 1987 (ESA SP-1094, October 1987).

One way to convince them is that, today and after this meeting we and you together form a solid lobby which has to achieve its full strength now if we are to succeed.

Certainly, it will be desirable to attract a greater number of earth scientists (I am thinking of oceanographers, geologists, etc.) and of well-qualified industrial firms. We are therefore counting on you to spread the word. In addition, we have decided to maintain continuous contact with the user community by repeating such meetings and, if necessary, to increase their frequency.

The detailed objectives of the Workshop will be outlined in Dr Pfeiffer's presentation. It is not my intent to duplicate on this aspect, but I should like to stress how important it is for us that we receive from you at the end of this Workshop answers to questions as:

1) Is the user community prepared to arrive at a consensus on a mission which has as a *primary* objective the precise determination of the Earth's geopotential fields?
2) What are your suggestions for the definition, the setting up and the management of the required data handling system?
3) How essential is the cooperation with NASA: (a) to the achievement of the mission objectives; (b) to the technical realisation of the system; (c) to the promotion of the programme, and (d) to the exploitation of the mission?

To conclude, I should like to repeat again that I can only prepare a Solid Earth Programme which is endorsed and supported by the large scientific community and which can be implemented within certain budgetary and programmatic constraints.

In all sincerity, I must say: it's now or never!

Matera Workshop discussions: Messrs B. Pfeiffer, P. Goldsmith, S. Hieber (ESA), and E.A. Finn (NASA).

WELCOME ADDRESS

Mr. Francesco Saverio Acito

Mayor of Matera

Ladies and Gentlemen,

I welcome all the participants in the ESA/NASA Workshop and also on behalf of the President of the Basilicata Region, Prof. Gaetano Michetti, who apologizes for not being here due to unforeseen circumstances.

It is with great pleasure that I welcome you to this little town in the Deep South in the hope that Matera will be up to its tradition as a hospitable town.

It offers a wealth of natural, artistic and cultural elements, the very presence of which should form a suitable background for creative activities. I sincerely hope that you will feel the warmth of our people and the pleasure of our sincere hospitality that are typical of our country.

Furthermore, thanks to CNR, Piano Spaziale Nazionale and in particular to the work of the late Prof. Colombo and to the support of the other friends of Lucania, among them Prof. Guerriero and Mr. Albanesi, Matero has now, besides its traditional elements: the 'Sassi', the 'Gravino', the rock-churches, left to us by the uninterrupted presence of the man from his prehistory up to today, other elements of international claim.

The cooperation among PSN, the Basilicata Region and the Municipality of Matera, made possible the realisation of a geodetic station, located a few kilometres from the ancient 'Sassi', which I hope will successfully accomplish the ambitious role given to it.

Hoping that Matera will be up to your expectations and that it will draw you back here, perhaps for a more relaxing stay, I express my best wishes for a successful meeting, a meeting to be remembered together with the name of our town that – and I make no secret about it – wants to become the 'Erice' of Geodesy.

Welcome again to Matera ... and good work!

Proceedings of an ESA-NASA Workshop on a Joint Solid Earth Programme, Matera, Italy, 29-30 April, 1987 (ESA SP-1094, October 1987).

WELCOME ADDRESS

Mr C Albanesi

Piano Spaziale Nazionale (PSN), Rome

Mr Mayor of Matera, Colleagues, Ladies and Gentlemen,

I feel very honoured and I am very pleased to welcome, on behalf of Piano Spaziale Nazionale (PSN) and of Prof. Luciano Guerriero, the participants of this meeting in which the most competent representatives of the international geophysics community are present.

Since 1983, when the station started its activity, many scientific and technical meetings have been held in Matera. This meeting, however, is particularly important as I feel confident it will give the opportunity to NASA, ESA and PSN, to lay the basis for future fruitful cooperations in the field of geophysics, a field which is assuming an ever-increasing importance for the high scientific and technological contents connected with its activities.

PSN, as you know, taking into account the rapid evolution of worldwide space activities, devotes great attention to future commercial applications as well as to technological frontier programmes in a large spectrum of fields such as telecommunications, propulsion, advanced structures, earth resources, remote sensing and scientific and technological research.

In this context, thanks also to NASA's support and full cooperation, PSN is developing ambitious activities in the field of geophysics, in the framework of the crustal dynamics programme.

PSN programmes in this field are in particular oriented towards the development of modern space techniques allowing the international scientific community to participate in measurement campaigns in the Mediterranean basin.

The focal point of this activity, and I say this with great satisfaction, is the Matera Station which has been realised with the efficient support of the Basilicata Region and of its authorities who, well aware of the importance of these programmes, contributed with great enthusiasm to the establishment of this centre.

Our best thanks to the Basilicata Region and to the Municipality of Matera for all their past and future support.

In particular, our appreciation and gratitude to the Mayor of Matera who, from the beginning, gave us his full collaboration in carrying out these strategic initiatives.

Our best thanks also to Telespazio, a company with a leading role in Italy in Earth Observation applications, which is responsible for the management of the station's operations.

The data collected by the Matera Station from the Lageos and Starlette satellites and lately from the Japanese geodetic satellite, are utilised for the setting up of more and more sophisticated mathematical models for the study of the Earth system.

In parallel, PSN is realising, with the involvement of Aeritalia and other industrial organisations, a second Lageos satellite which will greatly improve the present performance of worldwide observations.

Proceedings of an ESA-NASA Workshop on a Joint Solid Earth Programme, Matera, Italy, 29-30 April, 1987 (ESA SP-1094, October 1987).

In the near future the Matera Station will be equipped with a VLBI antenna, designed and realised by SeleniaSpazio and other qualified national industries, which will allow much more sophisticated measurements. Furthermore PSN is developing a mobile laser system with the involvement of CISE, Selenia and Galileo.

In the light of these ambitious programmes, the Matera centre will become a fundamental station: the use of advanced laser techniques and VLBI techniques allowing simultaneous measurements will enable a sinergy of interventions on a large scale and also on a regional scale.

The geodesy programme is the first important step: strategic plans are being jointly developed by PSN and the Basilicata Region with the support of University centres and industrial organisations.

Matera is therefore going to become an important centre for science and technology and will play an essential role in the promotion of initiatives in the geodesy and remote sensing fields.

The station will also assume the scientific and operational responsibility of all the multidisciplinary advanced activities which will be carried out in the Earth Observation field.

In conclusion I would like to say that all these activities will have full significance if they are developed with the consensus of the scientific communityy and with industrial involvement in the framework of cooperations with NASA and ESA which are PSN's most important partners for the definition and realisation of advanced programmes.

Thank you again and many wishes for a successful meeting which represents an important momentum for the identification of common strategies.

NASA's GEODYNAMICS PROGRAMME

D C McAdoo

NASA Hq, Washington, DC

GENERAL

Scientific Themes

- Dynamics of the Core
- Dynamics and Structure of the Mantle
- Dynamics and Structure of the Lithosphere
- Evolution and Composition of the Earth
- Comparative Planetology

Ongoing Projects

- Crustal Dynamics/Earth Observations
  - SLR, VLBI, GPS and LLR Observations
- Gravity Field Modelling
  - Interim Field, GEM T1
- Magnetic Field Studies

OFFICE OF SPACE SCIENCE AND APPLICATIONS (OSSA)

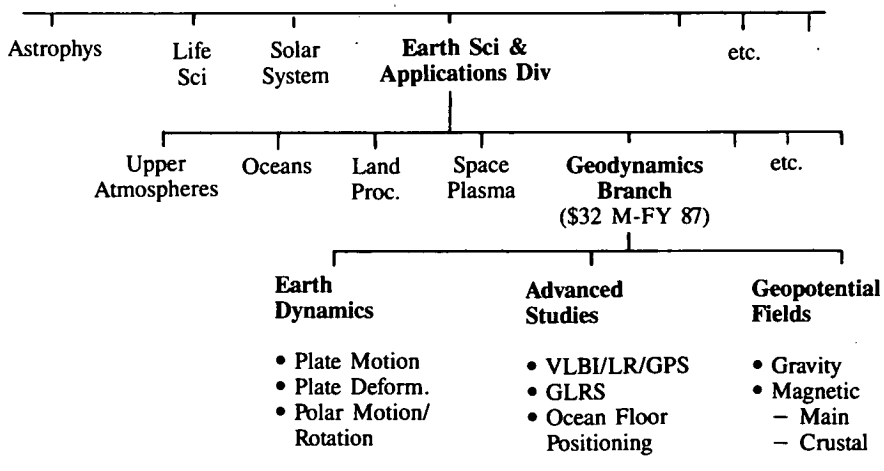

Proceedings of an ESA-NASA Workshop on a Joint Solid Earth Programme, Matera, Italy, 29-30 April, 1987 (ESA SP-1094, October 1987).

LAGEOS POLAR MOTION 1982.0–1986.0
5 day raw values

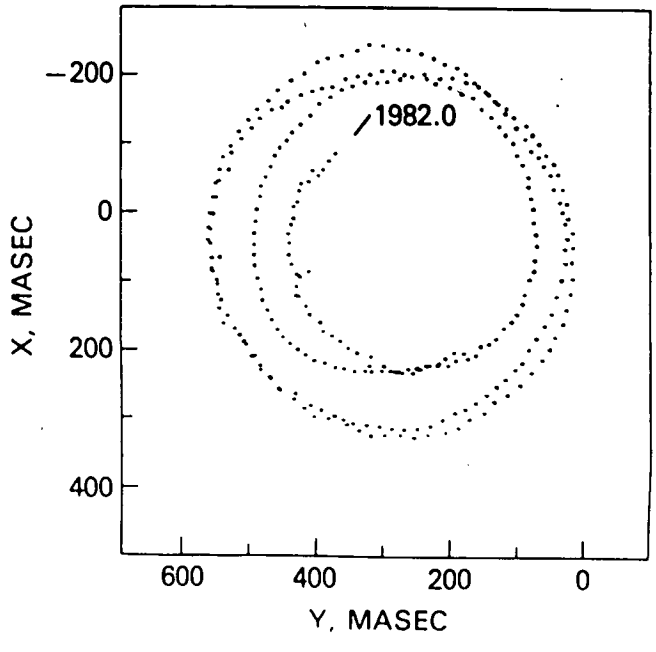

DETERMINATION OF j_2

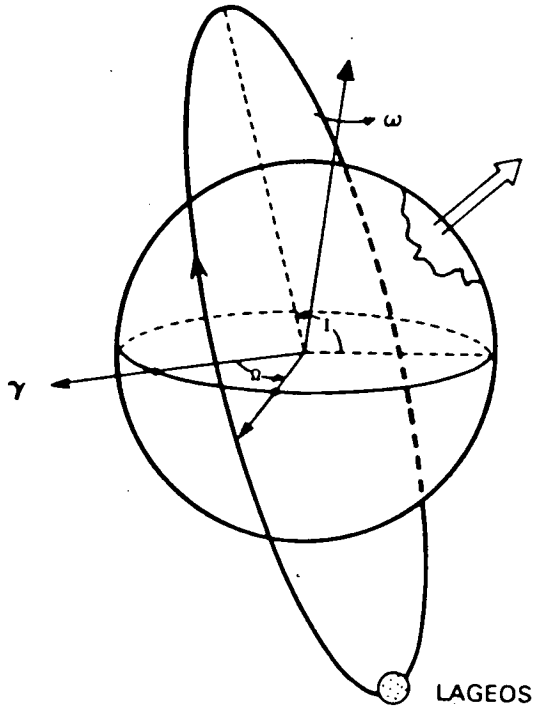

$$\dot{\Omega} \simeq -\frac{3}{2}\left(\frac{GM}{a^3}\right)^{1/2}\left(\frac{R_e}{a}\right)^2 J_2 \cos i$$

$$\ddot{\Omega} \propto j_2$$

GLOBAL MOTION VECTORS FOR SLR TRACKING SITES

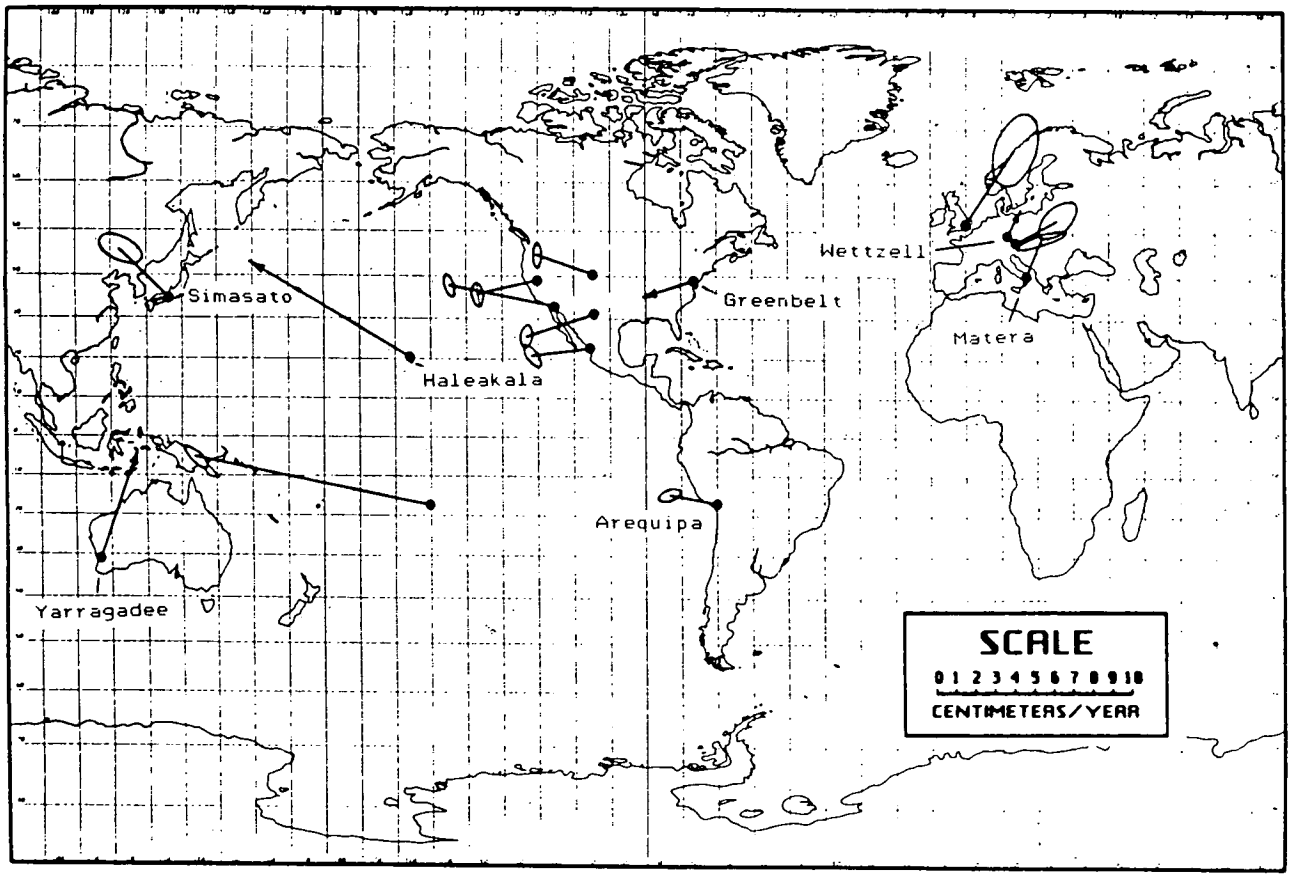

TECTONIC PLATE MOTION FROM YARAGADEE

To Station	Tetonic Plate	Observed Geodesic Rate (mm/yr)	AM1-2 Rate* (mm/yr)
Greenbelt, Maryland	North American	-80 ± 9	-89
Haleakala, Hawaii	Pacific	-91 ± 9	-103
Wettzell, W. Germany	European	-40 ± 4	-26
Simosato, Japan	?	-57 ± 5	-77
Arequipa, Peru	South American	65 ± 15	61

* Prediction based upon geologic rates (Minster and Jordan Jnl Geophys Rsch, '83, 1978)

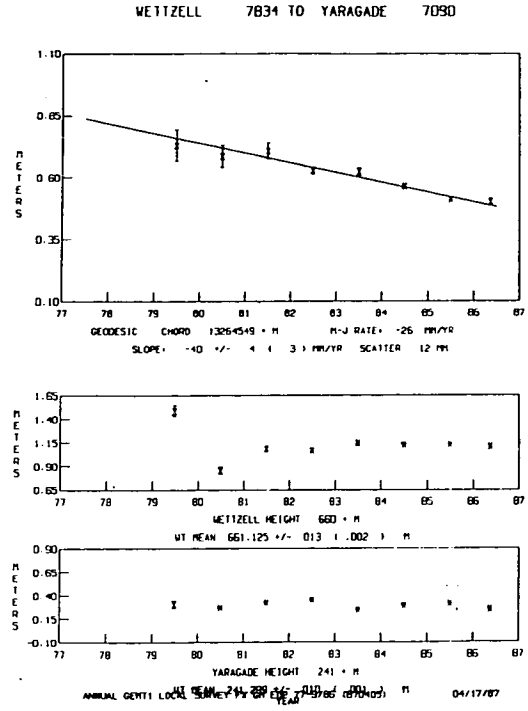

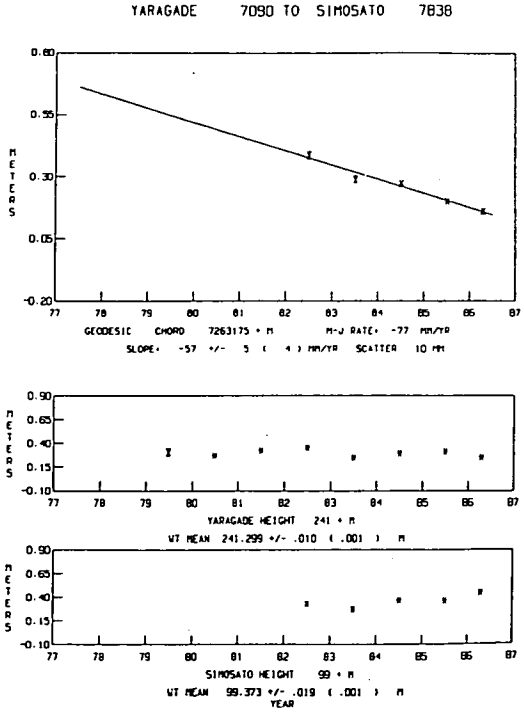

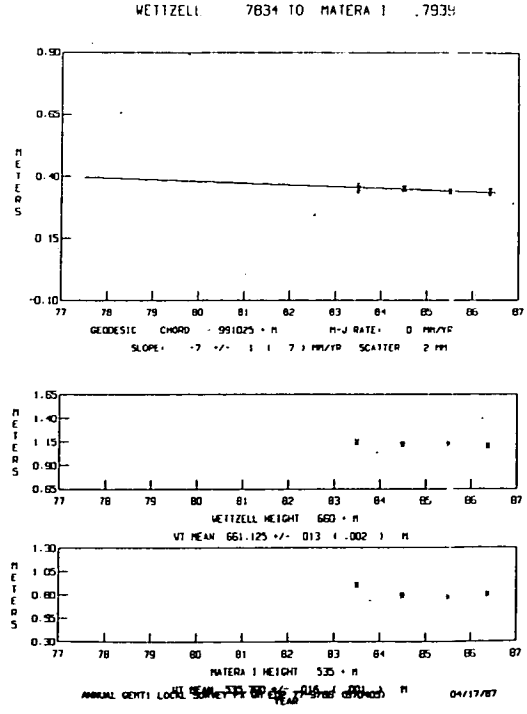

ORIGINAL PAGE IS
OE POOR QUALITY

GSFC GRAVITY MODEL OVERVIEW

- Multi-satellite only solution containing 17 satellites
- Gem-TI complete to (36,36)
- Solution for global ocean tides
- Solution for Earth orientation
- Overall improvement:
  - reduced rms of fit to tracking data
  - surface gravity comparisons
  - geoid
- Station coordinates:
  - preliminary laser solution
  - indicates consistency with apriori
- Calibration of errors

PRECISION ORBIT COMPUTATIONS FOR THE STARLETTE SATELLITE USING THE NOVEMBER 1986 GSFC EARTH GRAVITY MODEL

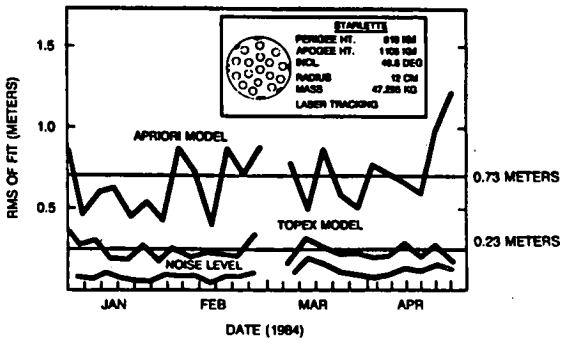

GSFC FUTURE PLANS FOR GRAVITY MODEL DEVELOPMENT

- ADOPT GEM-T1 FOR NEXT YEAR'S WORK (NEW A PRIORI)
- INCORPORATE ADDITIONAL DATA SETS:
  - ALTIMETRY--ALONG TRACK AND CROSSOVERS
  - SATELLITE TO SATELLITE TRACKING--GEOS-3/ATS-6, TDRSS/ERBS
  - COMPLETE MATRIX GENERATION FOR LASER SATELLITES
  - S-BAND AND OPTICAL DATA SETS (?)
- INITIATE EVALUATION OF SURFACE GRAVITY DATA
- CONTINUE TO REFINE THE CALIBRATION OF THE STATISTICS FOR GEM-T1 AND THE PREDICTION OF THE ORBIT ACCURACY PERFORMANCE ON TOPEX
- PERFORM STATION COORDINATE ADJUSTMENTS
- ATTEMPT TO PRODUCE AN IMPROVED MODEL BY FALL, 1987.

GEOIDS: from Spherical Harmonic Degrees 2 thru 6
Contour Intervals: 20 meters

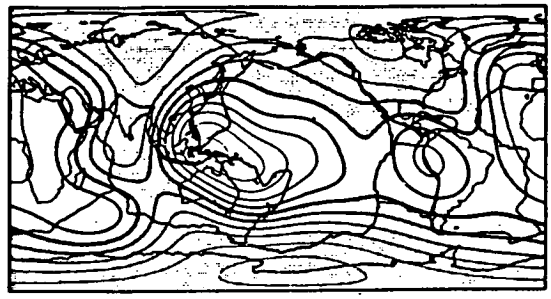

OBSERVED

OBSERVED MINUS SUBDUCTED SLAB EFFECTS

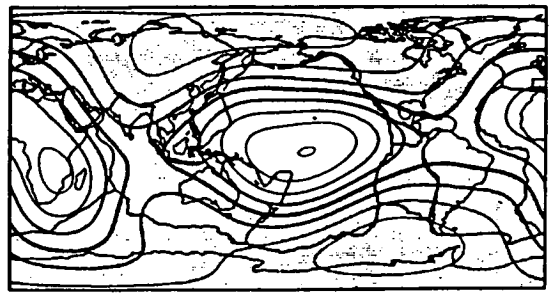

CALCULATED FROM SEISMIC VELOCITY VARIATIONS

Reprinted from Nature, Vol 313, No 6003, pp 541-545, 14 February 1985

GEOIDS from Spherical Harmonic Degrees 2 through 6.

MAJOR PLANNED SPACE FLIGHTS

- *Global Gravity/Magnetic Field Mapping – GRM (Geopotential Research Mission)*
  - 100 km resolution, 1 mgal/3 nT accuracy
  - mid 1990s
- *Main Magnetic Field & its Secular Change –MFE/Magnolia*
  - 5-yr duration, 1000 km resolution, 10 nT accuracy
  - Cooperative with CNES, early 1990s
- *Gravity Gradiometer Mission – SSGM*
  - 150 km resolution, ultra-high precision
  - late 1990s
  - Implications for relativity & planetary studies
- *Lageos II*
  - Cooperative with PSN
  - Early 1990s launch
- *Earth Observing System – EOS*
  - Spaceborne Laser/Altimeter
  - Eventually: Magnetics and gravity gradiometry
  - Late 1990s

Iris-Lageos II (Shuttle) ~ 1992/93.

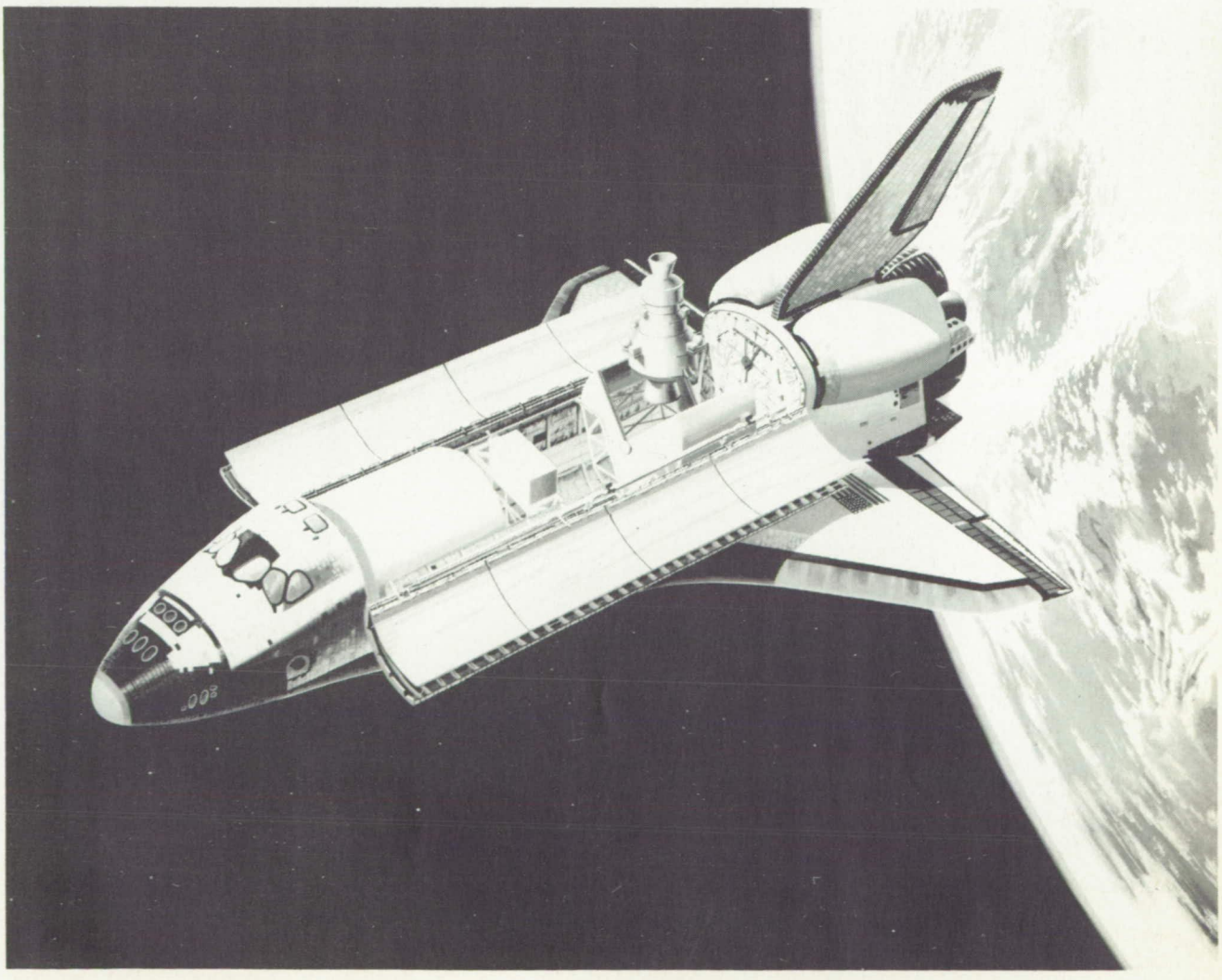

GEOPOTENTIAL RESEARCH MISSION (GRM)

BACKGROUND

- Recommended by ESSC as the next step after TOPEX in sequence of Earth System Science (ESS) missions
- Strongly recommended by 6 NASA and National Academy advisory committees
- Of major benefit to geophysics, geodesy and oceanography
- Complementary to TOPEX/POSEIDON

STATUS

- Candidate new start for FY1990
- NASA has strong interest in European cooperation which would enhance science objectives and reduce costs

SPACEBORNE MAGNETOMETRY

P T Taylor

NASA/GSFC, Greenbelt, MD, USA

Introduction

In October 1979 the first satellite designed to measure the near earth magnetic anomaly field was launched by NASA (Figure 1). This spacecraft had an elliptical orbit of some 560 to 350 km which slowly decayed over the satellite's seven month lifetime. Some fifteen non-U.S. investigators were part of the large group chosen to study these magnetic field measurements; many more researchers worked on these data as well (Langel and others, 1982). Since Magsat studies have begun, over two hundred and fifty publications have been written covering main and anomaly fields and external variations (Langel and Benson, 1987). This work has produced the best description of the main magnetic field ever published. Crustal anomaly work revealed the presence of long-wavelength anomalies which must have very deep sources. Magsat provided an important opportunity to study the magnetic field produced by external currents; especially the polar field aligned currents.

These scientific results were obtained from Magsat despite the fact that this satellite was in a relatively high earth orbit. At a lower orbit these results would be even more significant. In this report I will briefly discuss some aspects of future low-orbit (~160 km altitude) satellite magnetometer missions.

Lower-Altitude Mission

In order to ascertain the results from a lower-altitude magnetometer-bearing satellite mission, simulations of the field at lower altitudes and theoretical studies were undertaken. The latter will be discussed first.

Block models were used to determine the increase in resolution of lower orbiting satellites. Resolution is defined as the ability to distinguish two distinct magnetized blocks. A quantitative measurement of resolution is defined by the value of the highest amplitude anomaly over a block (A; Figure 2) minus the value between the blocks (B; Figure 2).

When this resolution factor is plotted versus altitude we can note the dramatic increase in resolution with decreasing altitudes (Figure 3). At Magsat altitude the resolution value is 0.6 while for the proposed GRM altitude of 160 km (Keating and others, 1986) the value is 10 which represents an increase of some sixteen times. At 240 km, the increase in resolution over Magsat is 3.3. For a more complete discussion which accounts for both distance between blocks, d (Figure 2), and block orientation see Schnetzler and others (1984).

Simulations of the anomaly field at any altitude can be made by continuing upward data measured at the surface. Since we must continue these data upwards hundreds of kilometers the area covered by these anomaly data sets must be large. In order to carry out these computations the data must be in digital form. Relatively few digital data sets of large regions are available. We have a digitized magnetic anomaly map of the United States. The U.S. magnetics upward continued to 160 km (Figure 4) is shown in comparison with a Magsat anomaly map of the U.S. at 3.2 km altitude (Mayhew and Galliher, 1982; Figure 5). A profile across the U.S. data at 160 km (Figure 4) is shown in Figure 6. Simulations were made in more detail. One of these detailed areas is located in the southwestern U.S. and is centered on the Rio Grande Rift (Figure 7). The Rio Grande Rift is seen as the northerly trending negative anomaly with a maximum amplitude of some -10nT.

These simulations and theoretical studies can only provide an indication of the magnetic anomaly field obtained at lower altitude, however, these studies suggest that significant new information can be found concerning crustal tectonic features. Since no magnetometer bearing satellites have traveled through the region of 160 km altitude this range of orbit height is virtually unknown in regards to external fields. While a mission at this altitude would represent frontier knowledge for external field studies, it represents a challenge for the crustal field researchers. The planned altitude of GRM, 160 km, (Keating and others, 1986) is located at the boundary between the ionospheric E and F regions. However, these regions vary with the local time and the level of sunspot activity. In the polar areas the activity is intensified by the presence of the field aligned currents whose return flow occurs at around 160 km altitude. This once again provides both an opportunity and an obstacle in the analysis of this low-altitude magnetic data.

While the main or core field magnetic researchers are pursuing their own high-altitude long-duration satellite mission (Magnolia/MFE; Bouzat and others, 1987) they will, doubtlessly, use these lower alti-

Proceedings of an ESA-NASA Workshop on a Joint Solid Earth Programme, Matera, Italy, 29-30 April, 1987 (ESA SP-1094, October 1987).

tude data to produce a time fixed or "snap-shot" model of the earth's main field.

It is apparent that a low-orbiting satellite carrying a magnetometer would be of great scientific value to not only those studying the crustal field of the earth but to external and main field workers as well.

Instrumentation

Like Magsat, this low-orbiting satellite mission should carry both vector and scalar magnetometers. The former will provide magnetic component measurements. Components are of value in crustal anomaly and main field modeling studies as well as being diagnostic indicators of external field variations. Two magnetometers will also provide internal consistency. While Magsat had a cesium scalar instrument it is uncertain at this time if a cesium or helium instrument would be preferable for future missions.

An important aspect of magnetic component measurement is the knowledge of the sensors attitude or rotational control or steering. Star cameras were used, together with an attitude transfer system, on Magsat. Recent advances in technology have led the way to non-magnetic star cameras. These newer devices would have the advantage of being situated near the magnetometers thus obviating the need for an attitude transfer system. Such star cameras are under development for the Magnolia/MFE mission (Bonzat and others, 1987).

In summary a lower altitude (~160 km) magnetometer-bearing satellite would be of great value for the study of the crustal anomaly and external fields and for main field modeling.

References

Langel, R.A., G. Ousley, J. Berbert, J. Murphy and M. Settle, 1982, The Magsat Mission, Geophyical Research Letters, v. 9, p. 243-245.

Langel, R.A. and B.J. Benson, 1987, Magsat Bibliography, NASA/GSFC Technical Memorandum 87822, 74pp.

Schnetzler, C.C., P.T. Taylor and R.A. Langel, 1984, Mapping Magnetized Geologic Structures from Space: The Effect of Orbital and Body Parameters, NASA/GSFC Technical Memorandum 80134, 19 pp.

Keating, T, P. T. Taylor, W.D. Kahn and F. Lerch, 1986, Geopotential Research Mission Science, Engineering and Program Summary, NASA/GSFC Technical Memorandum 86240, 209 pp.

Bouzat, C., G. Ousley and J. Runavot, 1987, Magnetic Field Explorer/Magnolia Joint NASA/CNES Phase A Study, 152 pp.

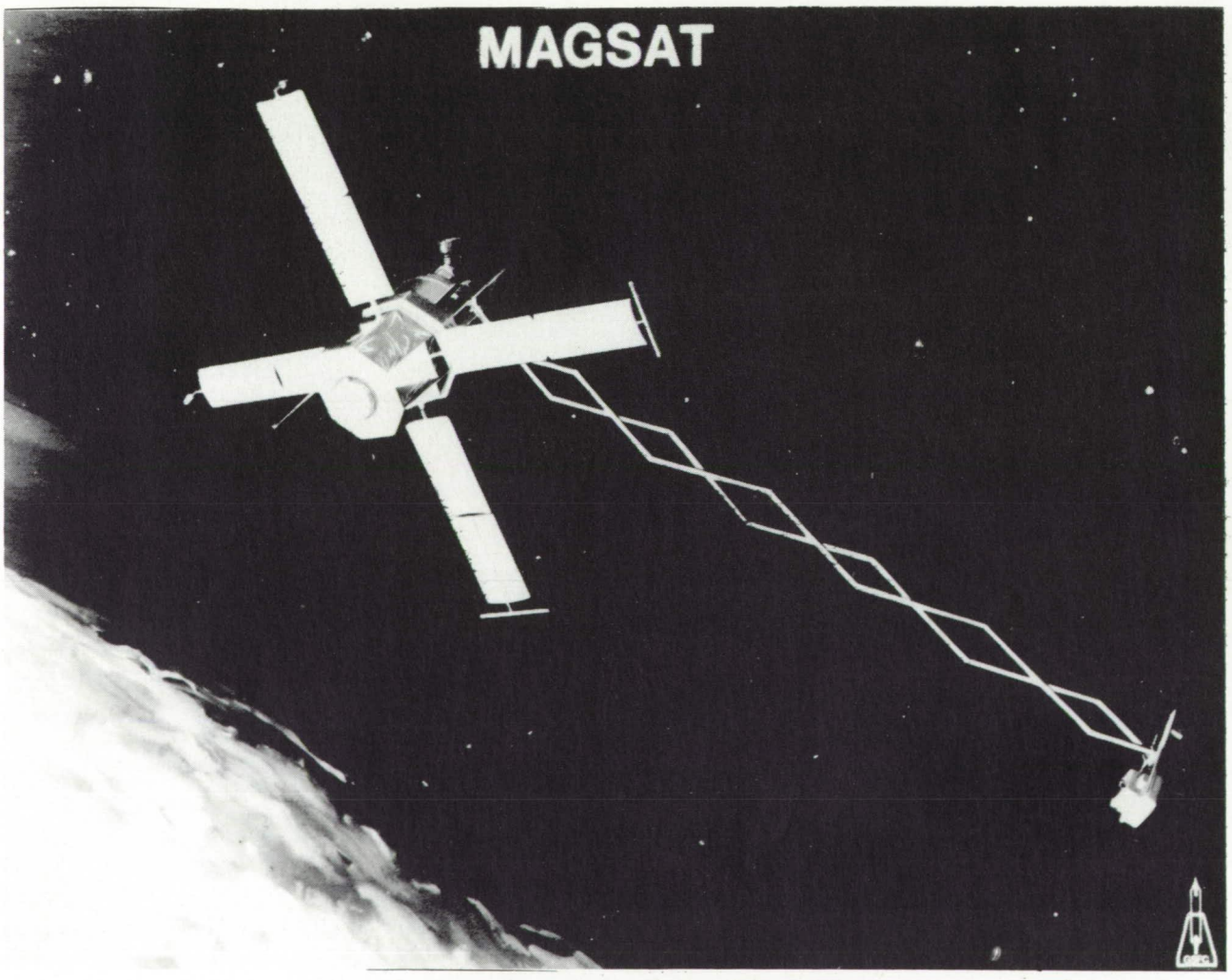

1. Artist conception of the Magsat mission.

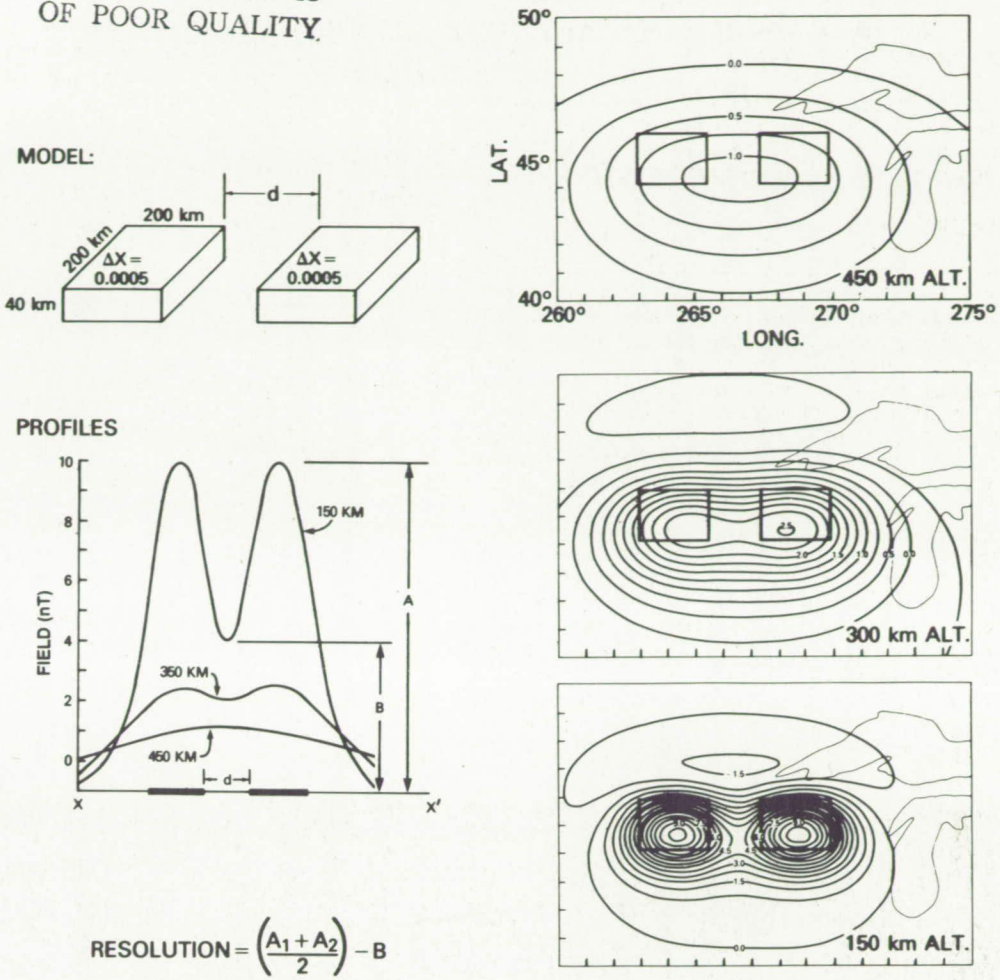

$$\text{RESOLUTION} = \left(\frac{A_1 + A_2}{2}\right) - B$$

2. Effect of altitude on resolution of magnetic bodies.

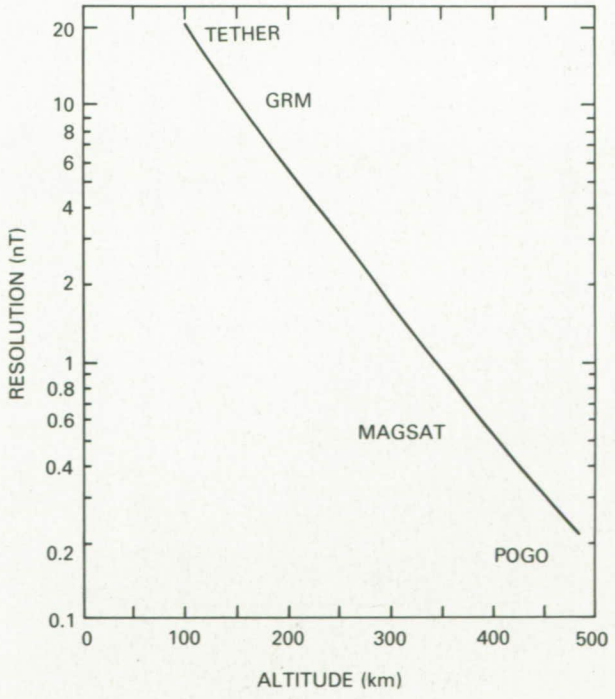

3. Resolution factor as a function of altitude.

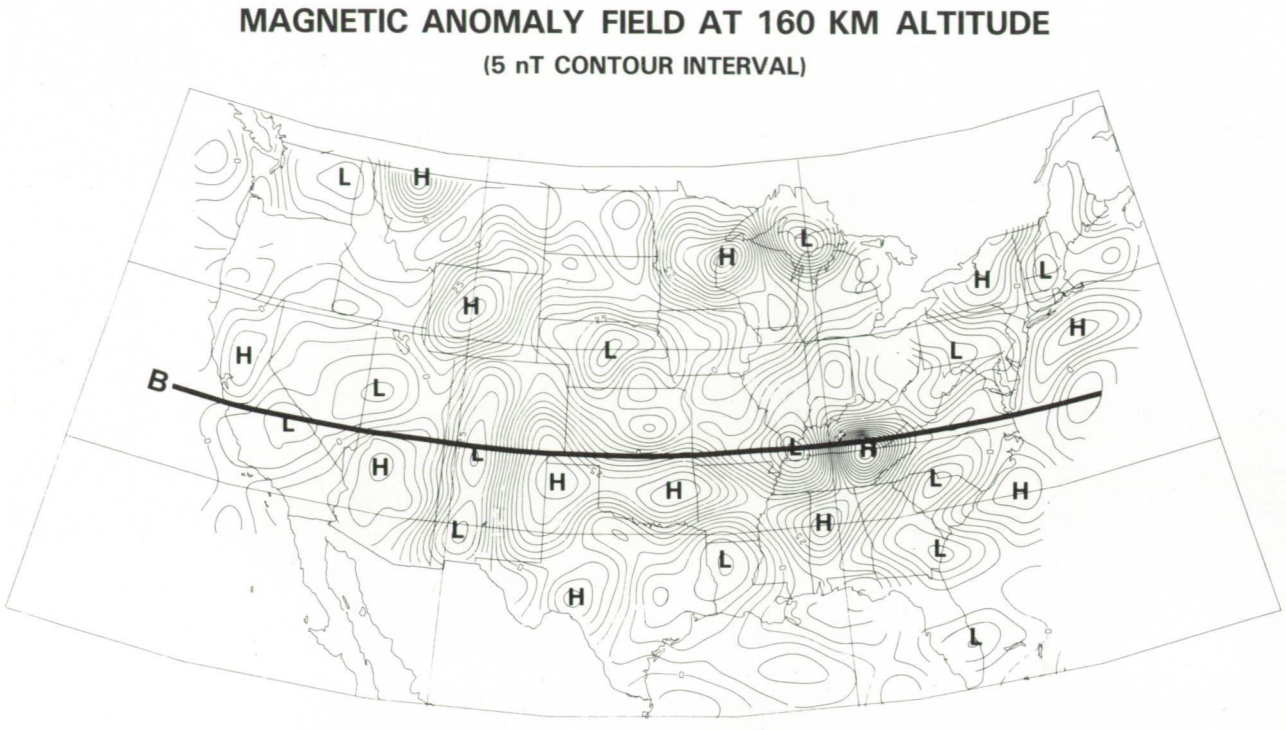

4. Simulated magnetic anomaly map of the United States for 160 km altitude. Contour interval in 5nT.

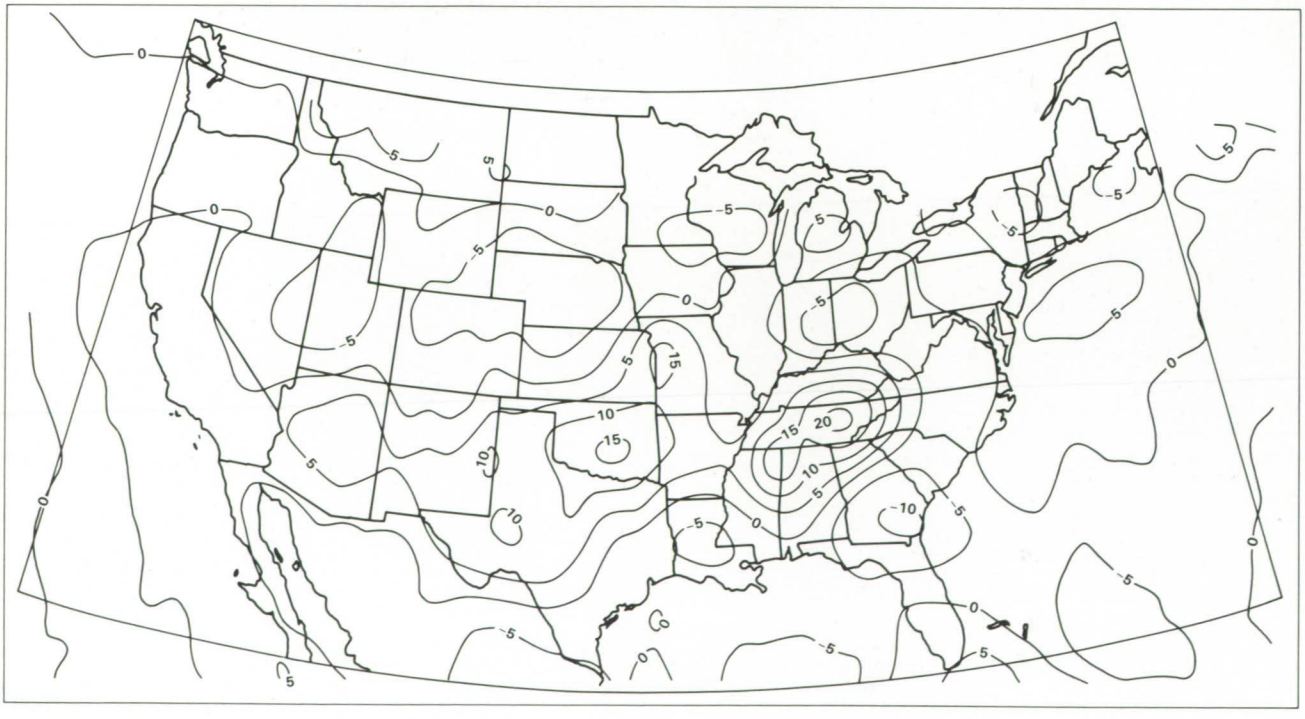

5. Equivalent source Magsat anomaly map at 320 km altitude. Contour interval is 5nT. (From Mayhew and Galliher, 1982).

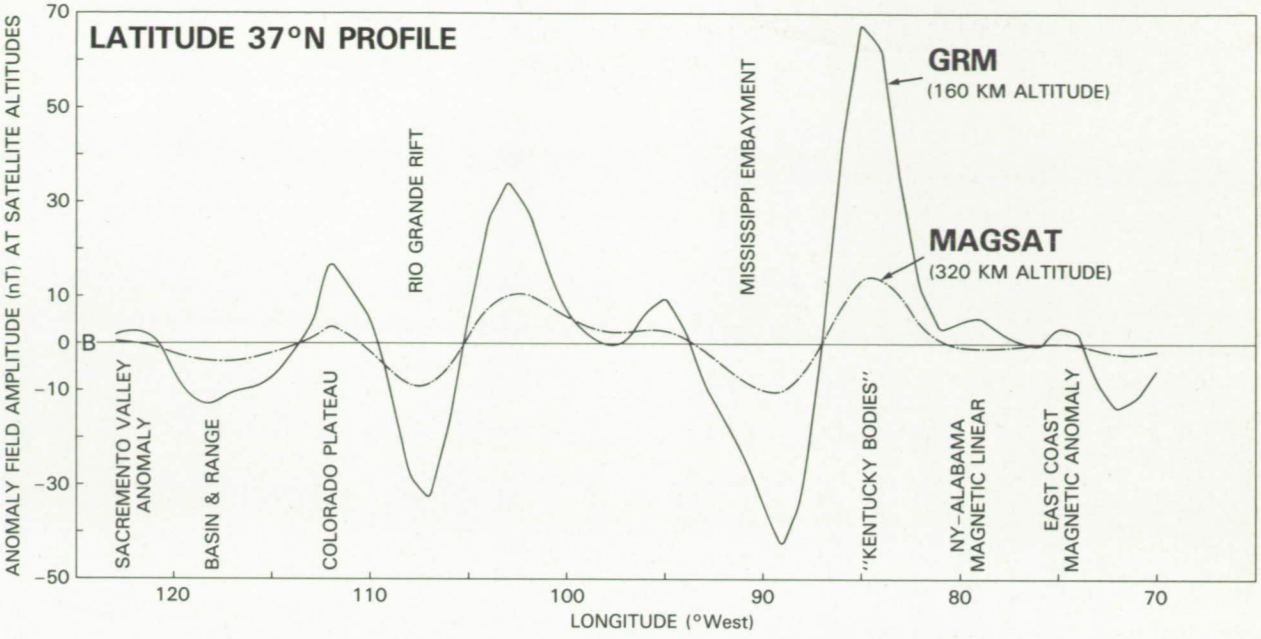

6. Profile through simulated U.S. data set (Figure 4) compared with Magsat data set (Figure 5). Note increases in both amplitude of anomalies (signal) and resolution over higher altitude data.

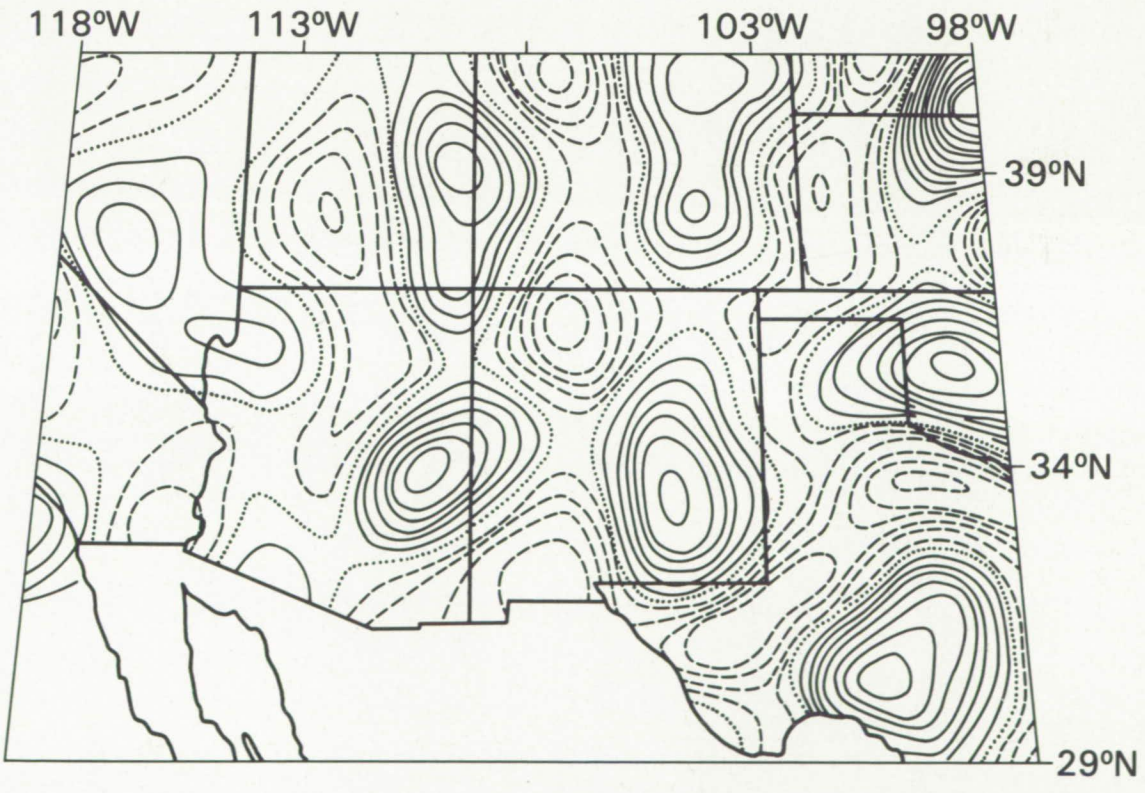

RIO GRANDE RIFT MAGNETICS c.i. 2 nT

BANDPASS (85 / 100 - 250 / 600) @ 160 Km ALTITUDE

7. Simulated magnetic anomaly field over the South Western U.S., contour interval is 2nT.

SPACEBORNE GRAVITY GRADIOMETRY CHARACTERISING THE DATA TYPE

D Sonnabend

JPL, California Inst. of Technology, USA

This paper is a general discussion of satellite gravity gradiometers, particularly covering the unique characteristics of this new data type. Since much of this derives from the unusual nature of the two stage drag free carrier vehicle, these ideas will be described first.

In a conventional drag free spacecraft (Slide 1), a spherical proof mass is free to move in a somewhat larger spherical cavity. When, due to external nongravitational forces, a collision with the proof mass appears imminent, spacecraft thrusters are fired to prevent it. Thus, the proof is free of everything but gravity, and, on average, so is the spacecraft. This permits great improvements in tracking accuracy, especially at low altitudes. For best performance, accelerometers comprising a gradiometer should be located symmetrically about the cavity. While zeroing the average acceleration is beneficial, the instantaneous values remain high, so that serious scale factor errors remain.

If carrier phase tracking is required, counted over times short compared to the thrusting intervals, then this arrangement is still not completely satisfactory. Within the GRM program, the problem led to the introduction of the two stage drag free shown in Slide 2. Here, an inner stage, carrying the tracking antenna(s), measures the relative position of the internal free proof mass, and feeds this to a set of magnetic forcers (MF), acting against the outer or main vehicle. As the external forces on the inner stage are low, and as the position relative to the proof mass is tightly controlled, carrier phase disturbances are greatly reduced. The corresponding advantage for a gradiometer, in lowering the instantaneous accelerations, was seen immediately; and this arrangement is now viewed as the only reasonable configuration for a low altitude gradiometry mission.

Next, I want to talk about a serious misconception concerning gravity gradiometers - that they measure gradient. Except for a perfectly inertially fixed instrument, this is not so. Instead, a perfect gradiometer measures components of what I call the intrinsic tensor, (Slide 3). The extra terms on the right are more or less equivalent to centripetal and coriolis terms in linear motion. Note particularly that no parameters of the instrument appear in this expression; so there's nothing the instrument designer can do about it.

So, how important are these corrections? (Slide 4) Assuming we can tolerate an error level of .001 Eotvos (1 E = 10^{-9} sec^{-2}), then the error in each correction must be below 10^{-12} $(rad/sec)^2$. Well, measuring angular acceleration at this level is just not done; so something besides direct measurement is needed. As for the angular velocity terms, if the instrument is controlled to be inertial, then the residual rate is of the order of the measurement error; and we could tolerate something like 10^{-6} rad/sec measurement and control error, which is practical with today's gyros. On the other hand, an earth pointing orientation for the instrument has several practical advantages. In this case, the nominal angular velocity is about .001 rad/sec, and the measurement requirement is pushed to 10^{-9} rad/sec, which is not practical with today's gyros.

Finally, although not directly connected with rate corrections, inertial attitude is needed to around 10^{-6} rad in order to permit an accurate transformation between instrument coordinates and some earth fixed reference coordinates in which the final potential calculations would be performed. Possible, but certainly not easy. Also, in connection with this same transformation, horizontal position is needed to a few meters. (Since Matera, I have come to understand that these latter requirements need only be enforced within the ground wavelength spectrum of interest.)

Proceedings of an ESA-NASA Workshop on a Joint Solid Earth Programme, Matera, Italy, 29-30 April, 1987 (ESA SP-1094, October 1987).

Over all, it appears that direct measurement of the rotation variables, followed by computed corrections to the intrinsic tensor, is not very practical. The instrument designers, particularly Alain Bernard and Ho Jung Paik, have suggested that relief from these problems is available by invoking the symmetry and tracelessness of the gradient tensor, together with the symmetry of the angular velocity terms and the asymmetry of the angular acceleration terms. They argue that certain combinations of matrix elements eliminate some of these rotation terms, thus avoiding the necessity of precise measurement. Further, by antisymmetrizing the intrinsic tensor, one is left only with the angular acceleration terms, which would greatly improve attitude determination. Personally, I am skeptical of these ideas, because noise, bias, self gravity, and other disturbances have no special symmetry properties, nor are they traceless.

However, I'm not here to cry doom, but rather to point out another way. What we have not used so far is the extremely strong dynamics of the nearly drag free inner stage. Slide 5, slightly modified from that shown in Matera, is the set of differential equations describing the motion of the inner stage. The first line is the Euler equations, describing angular motion from the viewpoint of coordinates fixed in the inner stage. The right side is the torque, consisting of aerodynamic effects on the protruding antenna(s), the control torques from the magnetic forcers, plus any other modelable torques such as self gravity. The second line is the kinematic equations. Euler parameters are assumed here, although this is not essential. The third line is the translational equations, relative to the proof mass. The right side specific forces correspond to the torque terms in the first line. Together, this is a system of 13th order.

This system, when augmented by measurements of the attitude and position, plus the Euler parameter constraint, plus estimates of the applied forces and torques, could be used to estimate the attitude variables needed to correct the intrinsic tensor. Since the forcing terms should be very accurately known, and the mass and the inertia tensor are relatively large, the estimates of the attitude variables should be far better than any measurements we could make. I have high hopes for this structure; but we have yet to begin an appropriate covariance study to determine what is achievable.

The power of this estimator can be further extended by including the gradiometer. To do this we need to add the gradiometer measurement model, which is the defining equation of the intrinsic tensor, as shown at the bottom of the slide. The dots at the right are for any known disturbances, such as self gravity. If we also add the symmetry and trace constraints, the whole solution should strengthen. Indeed, the entire strength of the Paik and Bernard techniques is automatically included in this estimate. Again, a considerable effort in setting up a covariance study will be needed before we can find out how accurately we can measure gradient, let alone the geopotential.

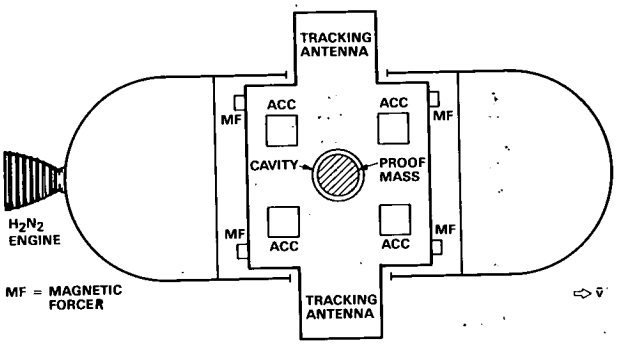

Figure 2: Two-stage drag free viewed from above.

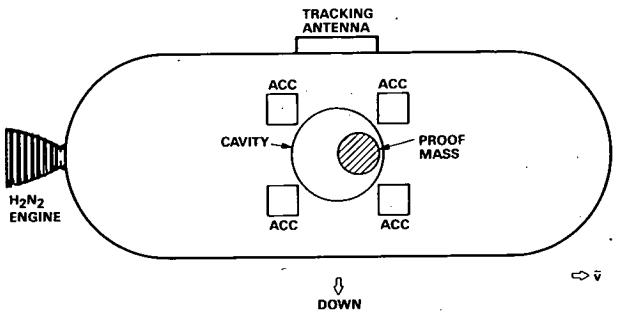

Figure 1: Conventional drag free.

$$T = H + \omega^2 I - \bar{\omega}\bar{\omega}^T + e\dot{\bar{\omega}}$$

H = GRAVITY GRADIENT TENSOR = $\nabla\nabla\phi$

I = IDENTITY TENSOR

$\bar{\omega}$ = INERTIAL ANGULAR VELOCITY

e = PERMUTATION TENSOR

Figure 3: The intrinsic tensor.

POSITION: For Rotation to Earth Coordinates

$|\delta\theta| < H_{TOL}/H_0 \sim 10^{-6}$ Radian

RATE: For ω^2 Corrections

Earth Fixed: $|\delta\omega| < H_{TOL}/\omega_0 \sim 10^{-9}$ Rad/Sec

Inertial: $|\delta\omega| < \sqrt{H_{TOL}} \sim 10^{-6}$ Rad/Sec

ACCELERATION: $|\delta\dot{\omega}| < H_{TOL} \sim 10^{-12}$ Rad/Sec^2

Figure 4: Rotation measurement accuracy.

Dynamic Constraints

$$J\dot{\bar{\omega}} + \bar{\omega}\times J\bar{\omega} = \bar{a}\times\bar{D} + \sum\bar{R}_i\times\bar{C}_i + \ldots$$

$$\dot{\bar{q}} = f(\bar{q}, \bar{\omega})$$

$$\ddot{\bar{r}} + 2\bar{\omega}\times\dot{\bar{r}} + \dot{\bar{\omega}}\times\bar{r} + \bar{\omega}\times(\bar{\omega}\times\bar{r}) = \frac{1}{m}(\bar{D} + \sum\bar{C}_i) + \ldots$$

Static Constraints

$$H^T = H, \quad \text{Trace } H = 0, \quad \bar{q}^T\bar{q} = 1$$

Measurements

$$T = H + \omega^2 I - \bar{\omega}\bar{\omega}^T + e\dot{\bar{\omega}} + \ldots$$

$$\bar{q}, \bar{r}, \bar{C}_i, \bar{\omega}(?)$$

Figure 5: Local gradient estimation.

TERRESTRIAL GRAVITY DATA AND COMPARISONS WITH SATELLITE DATA

R H Rapp

Ohio State University, Dept. of Geodetic Science & Surveying, Columbus, USA

Abstract

The collection of surface gravity data has grown slowly over the past ten years. Today there are estimates, based on actual observations, for 67% of the 64800 1°x1° equi-angular blocks. The standard deviation of these estimates is quite variable ranging from ± 1 mgal to ± 62 mgals. Areas for which direct observations are not available include China, Soviet Union, parts of South American, Africa, the polar regions, and portions of the oceans. Anomaly estimates for much of the ocean areas are available from satellite altimeter data to an accuracy on the order of ± 5 mgal from Geos-3 and Seasat data. Substantial improvement is not expected from ERS-1 nor TOPEX/POSEIDON on a global basis. There is good evidence that the terrestrial estimates are not independently determined. The correlation of the anomaly estimates complicates the use of such data in many problems if rigorous procedures are to be followed.

There are few areas of the world in which highly accurate 1°x1° mean anomalies are available. For example, there are 5361 1°x1° values (8% of the total possible) where the standard deviations are ≤ 4 mgals. Such areas are primarily in North America, Europe, and Australia.

Gravity anomalies dervied from satellite observations can be compared to the terrestrial estimates in several ways. One such procedure compares the two data types. For example, comparisons of a new NASA GEM T1 model which is complete to degree 36, to 5° equal area anomalies show that the satellite solution has an accuracy on the order of ± 4 mgal.

Other implied comparisons are made when the combination of satellite and terrestrial data are carried out. One finds that these are inconsistencies between satellite and terrestrial estimates of potential coefficients that can only be justified if the accuracy estimates on the terrestrial data are increased by about 2.5 times. Such problems may be related to the assumption of uncorrelated terrestrial anomaly data which appears not to be true.

For many studies it is important to obtain gravity information that is substantially more accurate that the data we now have, and distributed in a more global sense.

This presentation consists primarily of a set of figures that demonstrate the state of our terrestrial gravity coverage, and to show a few comparisons between satellite derived gravity field and terrestrial gravity data. The paper concludes with a set of references from which additional information can be found.

Terrestrial gravity is most often aggregated as 1°x1° mean free-air gravity anomalies. Categories of this data are kept at organizations such as the International Gravity Bureau, Defense Mapping Agency Aerospace Center (USA), and The Ohio State University. The number of values in such libraries has grown substantially in the past fifteen years, but many areas of the world remain without available gravity data because of geographic and political inaccessability. Figure 1 shows the location of terrestrial gravity data based on the June 1986 data base at Ohio State. Areas in which data is clearly missing includes the Soviet Union, China, parts of Africa, South America, Greenland and most of the polar regions. The available data in the polar regions is more clearly seen from Figures 2 (North Pole) and 3 (South Pole) regions.

Coverage maps do not tell the whole story because of the variable accuracy of the data. Figure 4 shows the location of 5361 1°x1° anomalies where the accuracy is equal to, or better than, ± 4 mgal. These more accurate anomalies cover 8% of the earth area.

From these figures, it is very easy to see that the accurate knowledge of the earth gravity field on a global basis is quite limited.

There has always been a great interest in the magnitude of agreement between the satellite gravity fields and the terrestrial gravity data. A number of ways have been developed to carry out this comparison recognizing that most satellite determinations of the gravity field are in the spectral sense, while the terrestrial data is given in a discrete or mean sense.

One recent comparison by Mainville and Rapp (1986) started in the spectral domain. In this case, the terrestrial data was converted to potential coefficients using orthogonality relationships. (In areas with no data,

Proceedings of an ESA-NASA Workshop on a Joint Solid Earth Programme, Matera, Italy, 29-30 April, 1987 (ESA SP-1094, October 1987).

anomalies computed from the GEML2 potential coefficient set were used). The difference between the GEML2 and terrestrial coefficients were computed in terms of anomaly differences up to degree 30. Figure 5 shows the location where the anomaly differernces exceeded 20 mgals. The circled areas represent locations where geophysically predicted anomalies were used as part of the terrestrial data. This figure shows a high correlation of large residuals and geophysical anomalies. It is important that actual gravity data, either by terrestrial or space technique, need to be acquired for these and other areas without reliable data.

Another mechanism for comparison can be found by computing the anomalies from the potential coefficients for comparison with terrestrial data. To make such comparisons the spectral content of each data type should be comparable. A recent comparison was described by Marsh et. al (1986) using the GEMT1 field, which is complete to degree 36, in comparison to anomalies derived from Seasat altimeter data at Ohio State. Figure 6 shows the mean square difference as a function of truncation degree for five different potential coefficient models. Of interest to us is the steady improvement of the T1 field, satellite above field, up to degree 32. Similar comparisons are needed for land gravity data. Results, such as shown by Marsh et. al indicate the value of independently determined gravity data for calibration and verification of geopotential models.

Another technique for comparing the satellite fields and the terrestrial data is to compute the spectrum of the differences, say in the anomaly domain. This was done in Rapp and Cruz (1986). They found that the differences were much larger than expected taking into account the assumed independent errors in the two data types. For example, at degree 20, the anomaly difference between the GEML2 and terrestrial field is 15.7 mgal^2, while one expects 6.7 mgal^2 on the basis of ±10 mgal 1°x1° anomalies. The large difference may be due to the neglect of the error correlation of the terrestrial data in the computations. More study needs to be done to take into account such correlations in solutions that combine terrestrial and satellite data as well as computations that use the terrestrial data to calibrate the satellite results.

The information presented here relates to our knowledge of the terrestrial gravity field and how such data interacts or compares with satellite derived gravity fields. In terms of accuracy coverage, only a few areas of the world have the information needed for geodetic and geophysical purposes. A gravity field mapping mission, with adquate accuracy and coverage, is a clear choice to improve our knowledge of the gravity field of the earth on a global basis.

References

Despotakis, V., The Development of the June 1986 1°x1° and the August 1986 30′x30′ Terrestrial Mean Free Air Anomaly Data Bases, Department of Geodetic Science and Surveying, The Ohio State University, Columbus, OH 43210, September 1986.

Mainville, A. and R. Rapp, Detection of Regional Bias in 1°x1° Mean Terrestrial Gravity Anomalies, in Bulletin D'Information, No. 57, Bureau Gravimetrique International, December 1985.

Marsh et al., An Improved Model of the Earth's Gravitational Field, GEM-T1, NASA, Goddard Space Flight Center, November 1986.

Rapp, R.H. and J.Y. Cruz, The Representation of the Earth's Gravitational Potential in a Spherical Harmonic Expansion to Degree 250, Report No. 372, Dept. of Geodetic Science and Surveying, The Ohio State University, Columbus, September 1986.

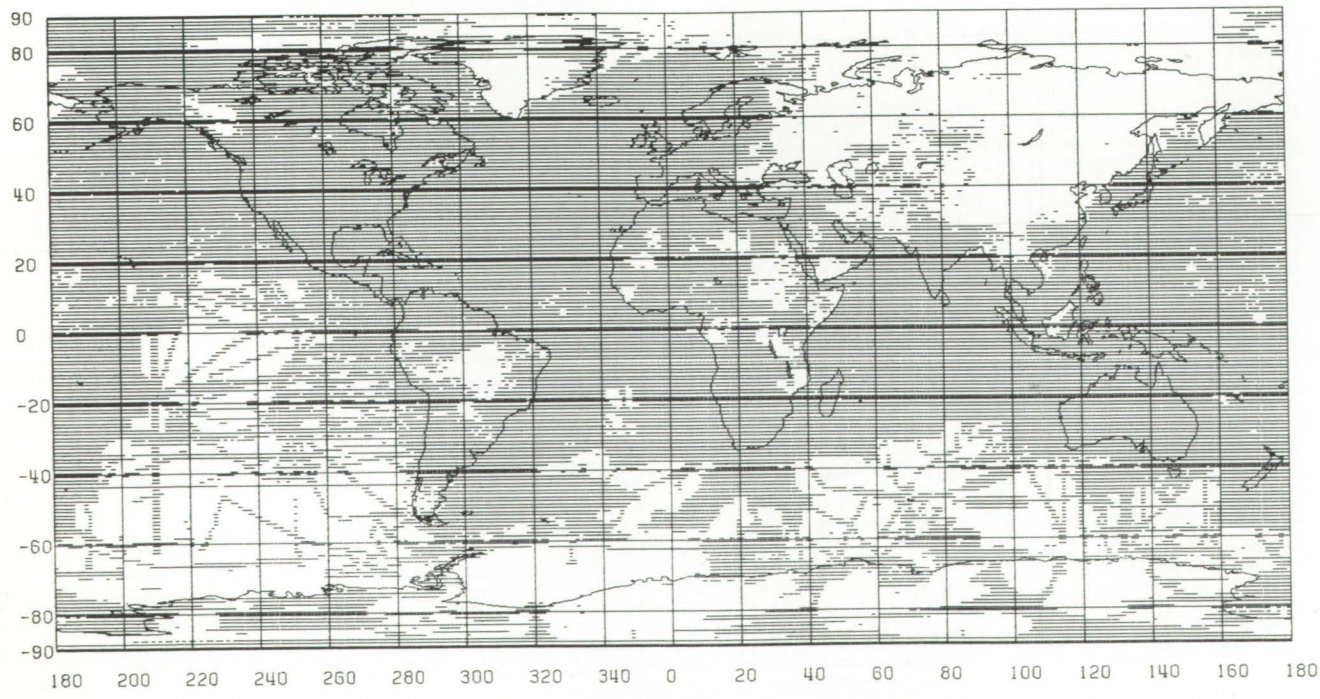

Figure 1: Location of 43271 1° x1° Mean Anomalies in the June 1986 OSU Field.

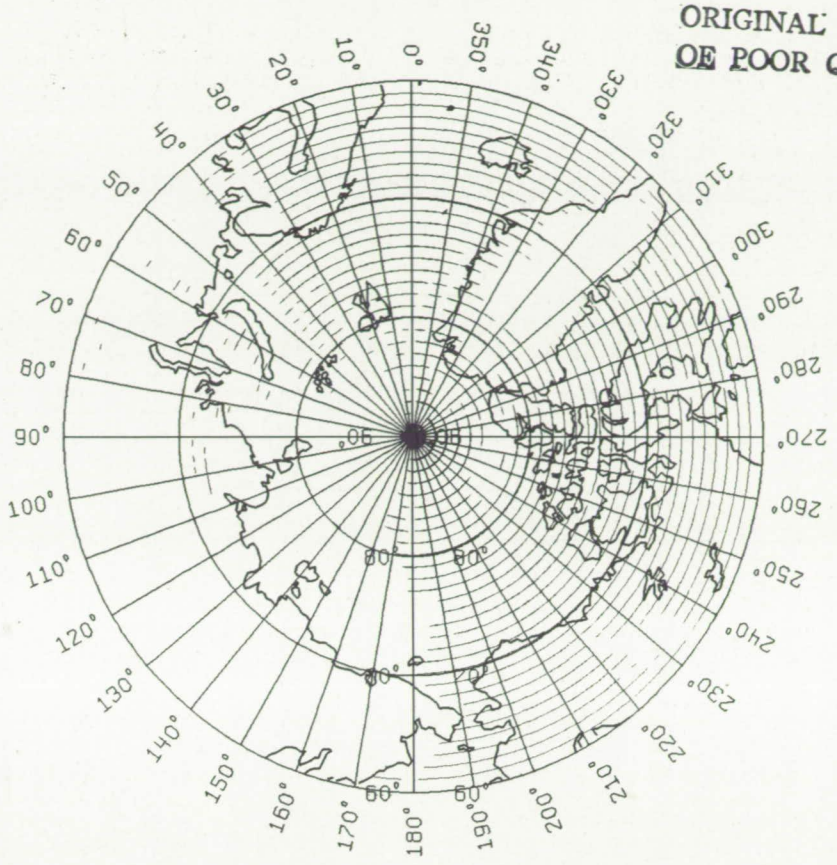

Figure 2: Location of 1° x1° Mean Anomalies in the North Polar Region, OSU June 86 Field.

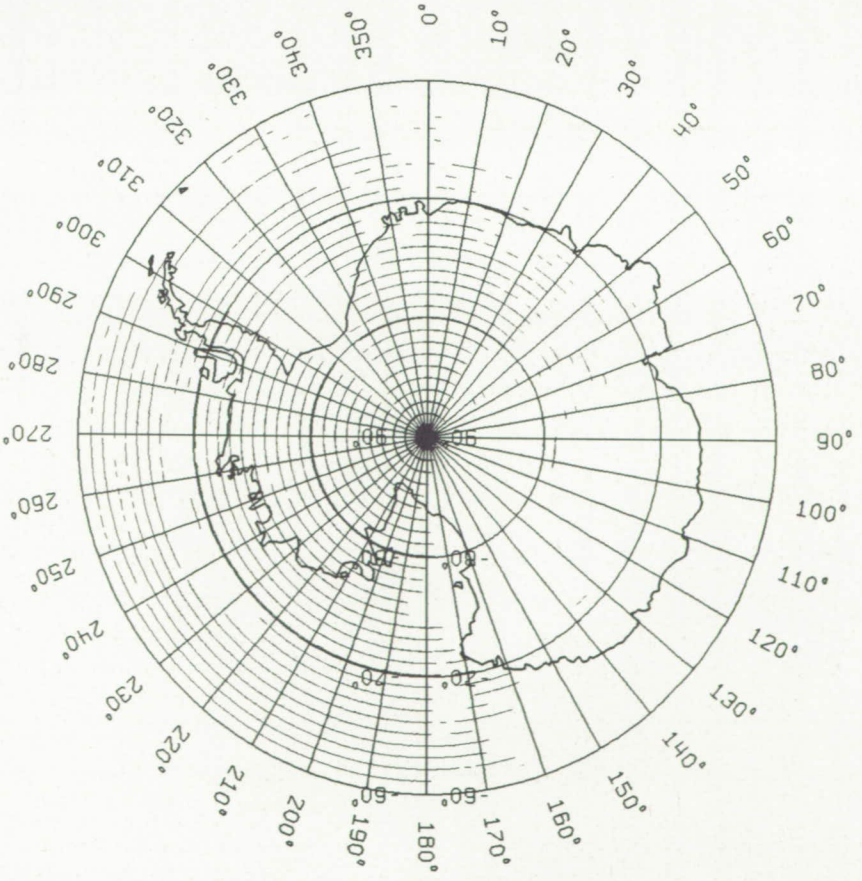

Figure 3: Location of 1° x1° Mean Anomalies in the South Polar Region, OSU June 86 Field.

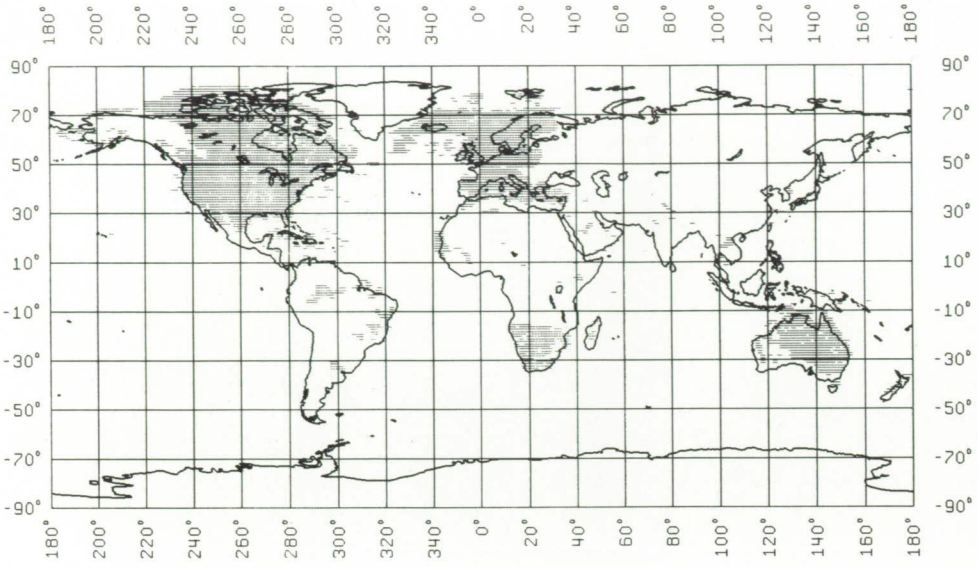

Figure 4: Location of 5361 1° x1° Mean Anomalies whose Accuracy is ≤ 4 mgals.

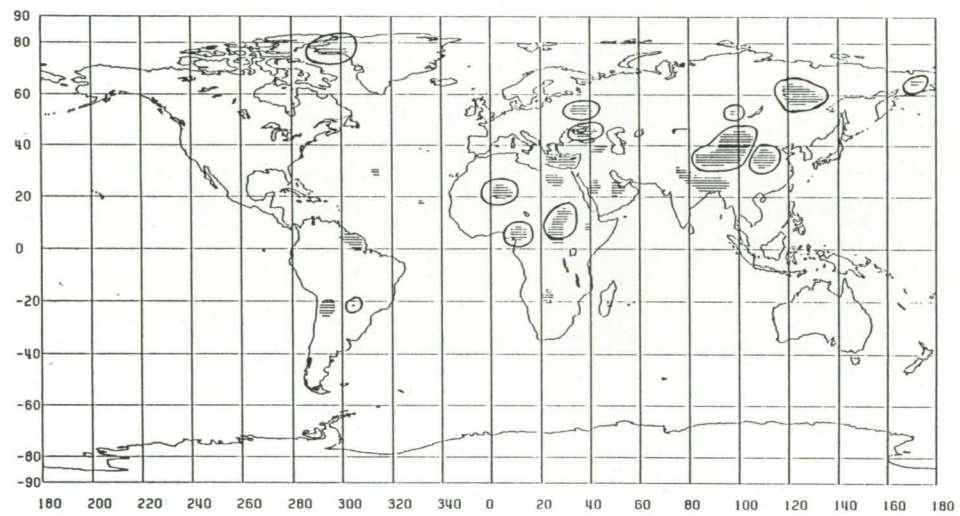

Figure 5: Location of 1° x1° Blocks where the difference between the Satellite Field and Terrestrial Field exceeded 20 mgals up to Degree 30.

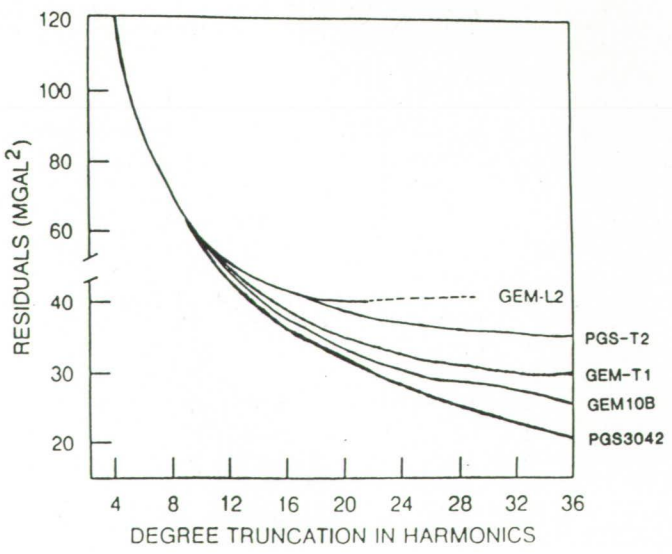

Figure 6 Mean Square Difference Between Potential Coefficient Derived 5° Anomalies and 1114 5° Anomalies Derived from Seasat Altimeter Data.

GRADIO THREE-AXIS ELECTROSTATIC ACCELEROMETERS

A Bernard

ONERA, Châtillon, F

ABSTRACT

Dedicated accelerometers are developed in ONERA for Satellite Gravity Gradiometry (GRADIO project). The design profits of the experience acquired with the CACTUS accelerometer, payload of the french satellite CASTOR-D5B (1975-1979) and with studies of highly accurate accelerometers for inertial navigation.

The principle of operation, based on a three-axis electrostatic suspension of a cubic proof mass, is well suited for the measurements of accelerations less than 10^{-4} ms^{-2}.

A resolution better than 10^{-11} $ms^{-2}/\sqrt{Hz}$ is expected.

1 - INTRODUCTION

Ground techniques and conventional satellite methodes cannot be used much further to improve the global accuracy and resolution of Earth gravity field models; It is now necessary to explore gravity variations in the resolution range of 50 to 200 km, over lands as well as over oceanic parts. Satellite Gravity Gradiometry (SGG) appears to be the most promising way to map the Earth gravity field at short wavelength.

An SGG project named GRADIO, based on differential micro-accelerometry, has been presented during the ESA Worshop SESAME ("Solid Earth Science and Application Mission for Europe"). As the basic principles of satellite Gravity Gradiometry were described there [1], this short note mainly presents the development of the dedicated three-axis electrostatic accelerometers for the GRADIO project.

2 - GRADIOMETY THROUGH DIFFERENTIAL ACCELEROMETRY: GENERAL PRINCIPLES AND REQUIREMENTS

2.1 - General principles

The purpose of the gravity gradiometer is to measure the second derivative tensor of the gravitational potential U:

$$t_{ij} = \frac{\partial^2 U}{\partial x_i \, \partial x_j}$$

[T] is a symmetric traceless tensor and therefore [T] has only five independent components.

The gradiometer consists of several non-coplanar ultra-sensitive three-axis accelerometers. For example, in the GRADIO project, eight accelerometers are located at the corners of a cubic structure, half a meter side. The differential measurement $\left(\vec{\Gamma}_j - \vec{\Gamma}_i\right)$ between two accelerometers is independent of the external force $\vec{F}_E$ acting on the spacecraft (resultant of the effects of the atmospheric drag and of the radiation pressures):

$$\left(\vec{\Gamma}_j - \vec{\Gamma}_i\right) = [A] \, \overrightarrow{O_i \, O_j}$$

with

$$[A] = [-T] + [\Omega^2] + [\dot{\Omega}]$$

where O_i and O_j are the centers of the accelerometers.

The antisymmetric part of the tensor [A] corresponds to the angular acceleration of the spacecraft:

$$[\dot{\Omega}] = \begin{bmatrix} 0 & -\dot{\Omega}_z & \dot{\Omega}_y \\ \dot{\Omega}_z & 0 & -\dot{\Omega}_x \\ -\dot{\Omega}_y & \dot{\Omega}_x & 0 \end{bmatrix}$$

The symmetric part of [A] contains the gravity gradient [T] and the centripital acceleration:

$$[\Omega^2] = \begin{bmatrix} -\left(\Omega_y^2 + \Omega_z^2\right) & \Omega_x \Omega_y & \Omega_x \Omega_z \\ \Omega_x \Omega_y & -\left(\Omega_x^2 + \Omega_z^2\right) & \Omega_y \Omega_z \\ \Omega_x \Omega_z & \Omega_y \Omega_z & -\left(\Omega_x^2 + \Omega_y^2\right) \end{bmatrix}$$

Proceedings of an ESA-NASA Workshop on a Joint Solid Earth Programme, Matera, Italy, 29-30 April, 1987 (ESA SP-1094, October 1987).

By use of linear combinations of the differential accelerometric measurements, it is possible to distinguish the antisymmetric part:

$$[\dot{\Omega}] = \frac{1}{2}\left([A] - [A]^T\right)$$

and the symmetric part:

$$[-T] + [\Omega^2] = \frac{1}{2}\left([A] + [A]^T\right)$$

The gravity gradient components, measured in satellite axes, must be provided in an Earth reference frame. M will denote the transformation matrix used for the change of coordinates. An Earth pointing is preferred for the satellite configuration and therefore, M is almost a unit matrix if the local orbital axes are choosen for the Earth reference frame. If X and Y correspond to the along track and cross track directions while Z is the vertical, the instantaneous angular velocity vector is then:

$$\vec{\Omega} = (\Omega_x \ \Omega_y \ \Omega_z)^T = (\delta\Omega_x \quad \Omega_0+\delta\Omega_y \quad \delta\Omega_z)^T$$

where $\Omega_0 \simeq 10^{-3}$ rad s^{-1} is the orbital angular frequency and $\delta\Omega_x$, $\delta\Omega_y$, $\delta\Omega_z$ are varying deviations which are assumed to be limited to 10^{-6} rad s^{-1} by the attitude control.

To a first order approximation and by taking into account the error [Δ] corresponding to the uncertainties on the spacecraft orientation and position, the measurement obtained from the symmetric part of the tensor [A] is given by:

$$\left[\frac{1}{2}\left([A] + [A]^T\right)\right]_L \simeq M^T\left([-T]_S + [\Omega^2]\right) M + [\Delta]$$

where: subindex L is for local orbital axes and subindex S is for satellite axes.

$$[\Omega^2] \approx \begin{pmatrix} -(\Omega_0^2+2\Omega_0\delta\Omega_y) & \Omega_0\delta\Omega_x & 0 \\ \Omega_0\delta\Omega_x & 0 & \Omega_0\delta\Omega_z \\ 0 & \Omega_0\delta\Omega_z & -(\Omega_0^2+2\Omega_0\delta\Omega_y) \end{pmatrix}$$

$$[\Delta] \approx -\frac{3GM}{r^4}\begin{bmatrix} \delta r & 0 & r\delta\theta_p \\ 0 & \delta r & -r\delta\theta_R \\ r\delta\theta_p & -r\delta\theta_R & -2\delta r \end{bmatrix}$$

r is the radius vector, GM is the product of the gravitational constant by the mass of the earth. $\delta\theta_p$ and $\delta\theta_R$ are deviations of the attitude in pitch and in roll. δr is the position error along the radius vector i.e. the vertical.

The gravity gradient components are not sensitive to first order to horizontal position and to the rotation about the vertical.

As [T] and [Δ] are traceless tensors, the trace of the measured tensor corresponds to:

$$-2\left\|\vec{\Omega}\right\|^2 \approx -2\left(\Omega_0^2 + 2\Omega_0\,\delta\Omega_y\right).$$

Thus, with a three-axis gradiometer, the disturbances due to $[\Omega^2]$ on the diagonal components of [T] can be corrected.

Furthermore, three linear combinations of these components are, to first order, independent of position and orientation errors:

$$\begin{matrix} T_{xx} - T_{yy} \\ 2T_{xx} + T_{zz} \\ 2T_{yy} + T_{zz} \end{matrix}$$

These combinations of the diagonal components are of special interest for the recovery of the gravitational field.

The determination of the non-diagonal components of [T] is not so directly achievable:

- variations of 10^{-2} Eötvös on T_{xy} and T_{yz} correspond to deviations of $\delta\Omega_x$ and $\delta\Omega_z$ of 10^{-8} rad s^{-1} only,
- the determination of T_{xz} (or of T_{yz}) is very sensitive to the unertainty on the pitch angle (or on the roll angle).

So the interest in a full tensor gradiometer is to provide all the information at a sensitivity level that can be reached only by the gradiometer itself: for example, the variations of the angular acceleration with a resolution of 10^{-11} rad s^{-2} through the antisymmetric part of the measured tensor. With independent observations, this information can be used in a global estimation process.

2.2 - Requirements

The accelerations due to the gravity gradient are in the order of 10^{-6} ms^{-2} with local variations less than 10^{-8} ms^{-2} while the greatest accelerations to undergo can reach 10^{-4} ms^{-2}. For example, if the gradiometer is rigidly fixed in the spacecraft, these accelerations correspond to the atmospheric drag at an altitude of about 200 km. At this altitude, the necessary sensitivity of the gradiometer is 10^{-2} Eötvös (i.e. 10^{-11} s^{-2}) to satisfy the scientific objectives of a gravity mission [2,3,4]. With a distance of 0.5 m between two accelerometers and with an averaging time of 4 s, the resolution of the accelerometers must be:

$$10^{-11}\ ms^{-2}/\sqrt{Hz}$$

That leads to a wide dynamic range of, at least 10^7.

In order to provide, in the differential measurements, the necessary rejection of the parasitic accelerations (from the external forces applied to the instrument and from its angular motion), the accelerometers must exhibit a good linearity, a low coupling between their three axes while very accurate scale factor matching and alignments have to be achieved.

3 - FROM CACTUS TO THE GRADIO ACCELEROMETER

The design of a dedicated accelerometer for GRADIO profits of the experience acquired at ONERA with the CACTUS accelerometer, payload of the french satellite CASTOR-D5B (1975-1979), and with the study of a highly accurate three-axis electrostatic accelerometer for inertial navigation.

The principle of operation of these accelerometers rests on the measurement of the force that is necessary to maintain a proof mass at the centre of a cage. This force is provided by a three-axis electrostatic suspension.

3.1 - CACTUS

The proof mass in CACTUS is spherical and made in a platinum-rhodium alloy. Its diameter is 4 cm and its mass is about 0.6 kg (Fig. 1).

During the whole life of the CASTOR-D5B satellite, CACTUS provided the measurements of the drag and of the radiation pressures from the Sun and from the Earth [5,6]. These results led to the design of a new version, so called SUPER-CACTUS, for the determination of the radiative budget of the Earth (BIRAMIS project studied under ESA contract) [7,8].

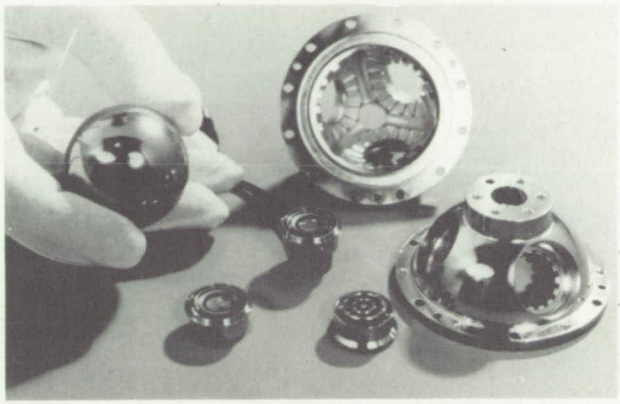

Fig. 1.

CACTUS: the proof mass, the cage in two parts and the systems of electrodes of the electrostatic suspension.

Fig. 2.

ONERA's drop tower facility: the capsula used for the tests of CACTUS.

Especially designed for space applications, CACTUS had a measurement range from 10^{-10} ms^{-2} to 10^{-4} ms^{-2}. So, this accelerometer could not operate on ground, under normal gravity conditions. Before satellite integration and launch, the only global tests performed on CACTUS were done in the ONERA's drop tower facility. During these tests, the accelerometer was mounted at the centre of the capsula shown in Figure 2.

The tower, Figure 3, is 42 m high and it allows a drop of 3 s into vacuum (10^{-5} Torr) during which the accelerations applied to the accelerometer corresponds to the residual disturbances on the capsula (drag, eddy currents,...). These accelerations are as low as a few 10^{-8} ms^{-2} in the horizontal plane.

3.2 - Three-axis electrostatic accelerometer for inertial navigation

A very high level of sensitivity, 10^{-10} ms^{-2}, has been obtained with CACTUS. Since then, the development of the accelerometer for inertial navigation has shown that a high accuracy can also be insured with a three-axis electrostatic suspension. The proofmass must be kept motionless

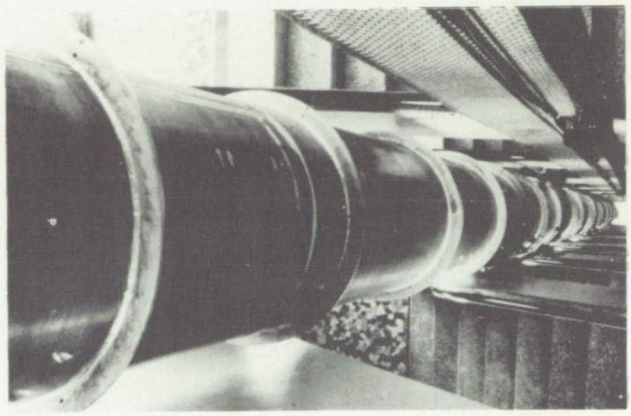

Fig. 3. ONERA's drop tower facility.

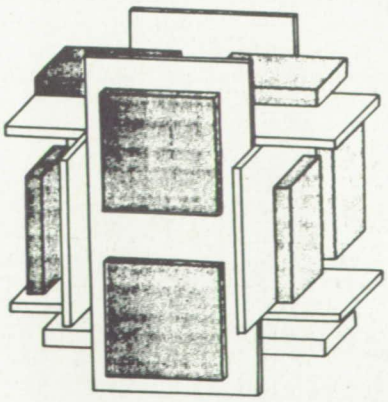

Fig. 4. Electrode arrangement around the cross-shaped proof mass of the accelerometer for inertial navigation.

and contactless in front the electrodes. The control of its six degrees of freedom (three translations and three rotations) is achieved by means of six pairs of electrodes (Fig. 4) simultaneously used for capacitive position sensing and for applying the restoring electrostatic force and torque [9].

For the proof mass and the electrode set, gold plated silica parts are used in order to minimize thermal expansion errors and to obtain a high stability of positioning.

Because the accelerations to undergo for inertial navigation are in the order of 10 G (1 G $\approx$ 9.8 ms^{-2}), high voltages are necessary for the suspension. To limit these voltages to $\pm$ 1000 V, small gaps between electrodes and proof mass and a high surface to mass ratio for this one had to be obtained. The cross-shaped proof mass, made in silica, has a mass less than 1 g while presenting 6 plates, each of 2 cm^2 at a distance of 40 μm from the electrodes.

The on ground testing of this three-axis electrostatic accelerometer is no longer a problem. As the drifts of the capacitance pick-offs are quite negligible, thus keeping the proof mass centred with respect to opposite electrodes, the biases are very stable and their thermal sensitivity is less than 10 $\mu G/°C$. Changes of scale factors versus temperature are more important because the restoring forces strongly depend on the distance between the electrodes and the proof mass. Relative variations of about $5.10^{-5}/°C$ are obtained. They correspond to changes of $10^{-3}\mu m/°C$ only of the gaps of 40 μm.

4 - THE GRADIO ACCELEROMETER

4.1 - Principles of operation

For gravity gradiometry, high sensitivity and high accuracy are both required. The principles of operation of the GRADIO accelerometers are the same as for the navigation three-axis accelerometer but the design takes advantage of the low levels of acceleration to undergo (less than $10^{-5}G$) for the optimization of the performances.

Instead of the very light cross-shaped proof mass previously described, a solid cubic proof mass is used for the GRADIO accelerometer.

The electrostatic forces remain normal to the faces of this cube and thus these directions determine the sensitive axes. The use of a gold plated optical cube, made in silica, with parallelism and orthogonality deviations less than 10^{-5} rad, insures a very low coupling between the three axes.

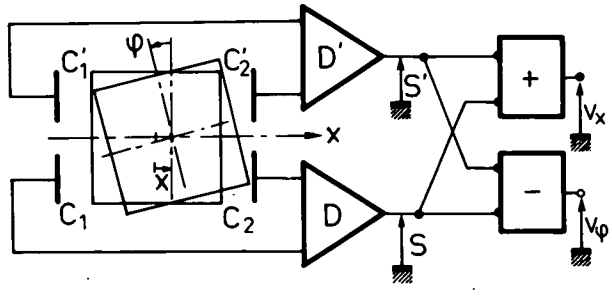

Fig. 5. Position sensing: translation S + S' → x; S − S' → φ.

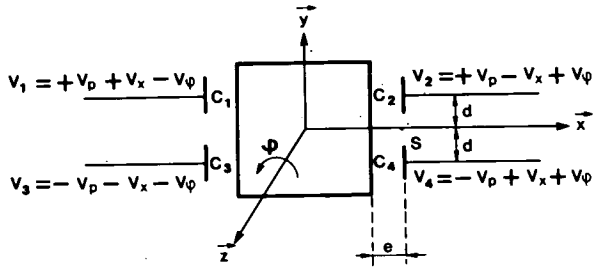

Fig. 6. Linear combinations of control voltages applied between the electrodes and the proof mass.

The electrostatic suspension of this cubic proof mass is achieved by three servocontrol channels acting separatly along the three axes of the accelerometer.

As shown in Figure 5, for each axis, the position sensing is provided through two pairs of electrodes by two capacitance pick-offs: the sum of their outputs leads to the linear deviation x while the difference corresponds to the angular deviation φ.

The electrostatic suspension is achieved by applying, between the proofmass and the same set of electrodes, the combinations of D.C. control voltages as it is shown in Figure 6. The carrier frequency and the selectivity of the capacitance pick-offs are high enough to allow such a superimposition.

The attractile force exerted by each electrode is a quadratic function of its voltage difference with respect to the proofmass:

$$\vec{F}_i = \frac{1}{2} V_i^2 \overrightarrow{\nabla C_i} \quad \text{with} \quad \overrightarrow{\nabla C_i} = \left[\frac{\partial C_i}{\partial x} \frac{\partial C_i}{\partial y} \frac{\partial C_i}{\partial z}\right]^T$$

For the electrodes of axis $\vec{x}$ for instance:

$$\overrightarrow{\nabla C_i} \approx - \frac{\epsilon S}{e^2} \vec{x} \text{ for } i = 1 \text{ and } i = 3$$

$$\overrightarrow{\nabla C_i} \approx + \frac{\epsilon S}{e^2} \vec{x} \text{ for } i = 2 \text{ and } i = 4$$

where S is one electrode surface, e is the gap between electrodes and proof mass and ϵ is the permittivity ($\epsilon \approx 8.85 \times 10^{-12}$).

With a symmetrical configuration and a centred proofmass, the electrostatic force along $\vec{x}$ and torque about $\vec{z}$ due to the two pairs of electrodes, Figure 6, are expressed by:

$$F_x = - \left[\frac{4\epsilon S}{e^2} V_p\right] V_x$$

$$N = - \left[\frac{4\epsilon S}{e^2} d\, V_p\right] V_\varphi$$

where V_x and V_φ are the control voltages for translation and rotation and d is the electrode lever-arm.

Thus, the bias voltages $\pm V_p$ insure linear characteristics for the control and therefore for the accelerometer.

The measured deviations x and φ are the inputs of two P.I.D. controllers whose outputs, V_x and V_φ, correspond to the following linear combinations:

$$V_x = a_x\, x + b_x\, \dot{x} + c_x \int x\, dt$$

$$V_\varphi = a_\varphi\, \varphi + b_\varphi\, \dot{\varphi} + c_\varphi \int \varphi\, dt$$

The coefficients are determined in such a way as to obtain the desired bandwidth and damping ratio. In steady state, the integral controls nullify the deviations.

Along each axis, the accelerometric measurement is provided by the translation control voltage V_x (or V_y or V_z) while the scale factors are $\left[\frac{4\epsilon S}{me^2} V_p\right]$, m denoting the mass of the suspended cube.

4.2 - Laboratory model configuration

The present studies aim at the pre-development of the GRADIO accelerometer with laboratory models that can be tested on ground under normal gravity conditions. The choosen configuration of these models is shown in Figure 7.

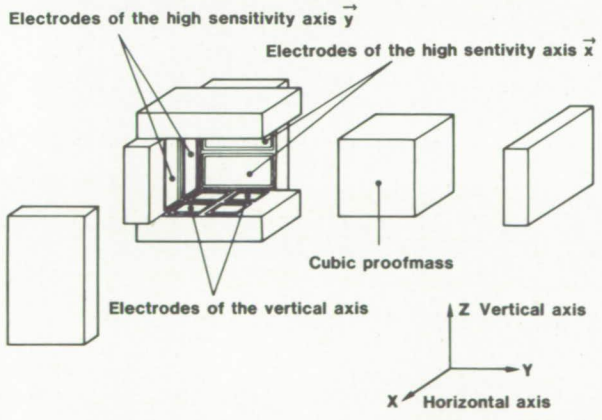

Fig. 7. Laboratory model configuration.

Four pairs of electrodes are used for the vertical axis which has to undergo a one G acceleration. This makes it possible to control not only the vertical translation but also the two rotations about the horizontal axes. Then, the sensitivity of these axes can be increased to the level allowed by the parasitic accelerations in the laboratory conditions.

Each horizontal axis has two pairs of electrodes and their configuration is such (see Figure 7) that only one of them, the $\vec{y}$ axis,

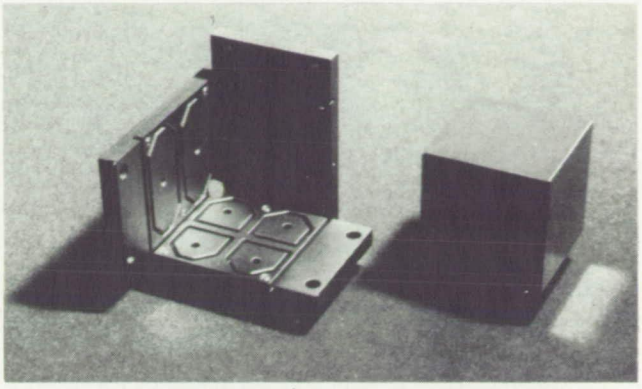

Fig. 8. Gold plated silica parts of the laboratory model.

controls the rotation about the vertical axis. Thus, eight pairs of electrodes and eight capacitance pick-offs are available to control six degrees of freedom only. This leads to a redundancy and the two supplementary sensors are used to test, with a very high accuracy, their drifts as well as the stability of the mechanical assembly.

The gold plated silica parts used for the proofmass and for the electrode set are shown in Figure 8.

The simplicity of the shapes is well suited for grinding and ultrasonic machining.

The increased sensitivity of the horizontal axes is obtained by using large gaps between the electrodes and the proof mass (400 μm instead of 30 μm for the vertical axis) and by lowering the bias and control voltages. The present range of these axes is 10^{-3} G to 10^{-10} G.

A first step has been done in 1986 with the suspension of an hollow cubic proof mass whose mass was 12 g. The suspension of a solid cubic proof mass, 3 cm side and 70 g, has been successfully achieved in February 1987 and since then, two laboratory models have been built to be tested in a differential mode.

The whole mechanical part, with the low level electronics integrated around it, is shown in Figure 9. The suspension of the proof mass is achieved into vacuum that is maintained with the ionic pump fixed on top of the model.

It appears impossible to provide an on ground testing of the accelerometer at the level of sensitivity required for satellite gravity gradiometry (dynamic range from 10^{-4} ms^{-2} to 10^{-11} ms^{-2} i.e. about 10^{-5} G to 10^{-12} G). Thus, the flight models, in their ultimate configuration, will have to be tested in the ONERA's drop tower facility as it was done for the CACTUS accelerometer.

The theoretical limit of the accelerometer resolution corresponds to the thermal noise in the low level electronics of the capacitance pick-offs. Through the negative stiffness introduced by the bias and detection voltages, that would lead to a resolution of

$$10^{-12}\ ms^{-2}/\sqrt{Hz}$$

for the accelerometer.

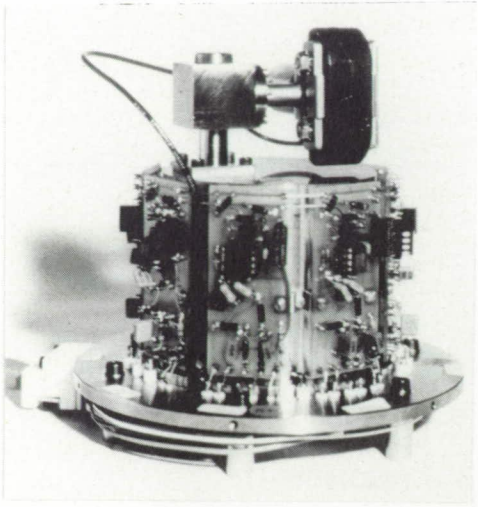

Fig. 9. Mechanical part of the laboratory model equipped with the low level electronics and with its ionic pump.

5 - DIGITIZATION AND ON-BOARD CALIBRATION

With this resolution and a full scale of 10^{-4} ms^{-2}, the dynamic range of the accelerometer would be 10^{8}. A voltage to frequency conversion of the analog accelerometer outputs is well suited to cover such a wide dynamic range because the measurement bandwidth is limited to very low frequencies: the maximum resolution will be obtained with an integration time of 12 s. One channel for each accelerometer axis provides the necessary data for the measurement and for the calibration processing described hereafter.

To take advantage of the high resolution provided by the GRADIO accelerometers, their sensitivity errors must be corrected. The accelerometric measurement of the acclerometer "i" can be written as:

$$\vec{\Gamma}_i = ([I] + [\epsilon]) \left[\left([-T] + [\Omega^2] + [\dot{\Omega}] \right) \vec{OO}_i + \frac{\vec{F}_E}{M_S} \right]$$

where [I] is the unit matrix, $\vec{OO}_i$ denotes the location of the accelerometer "i" and M_S is the mass of the satellite. [ϵ] is the matrix of sensitivity errors:

- the diagonal components of [ϵ] are scale factor deviations which can be as large as 10^{-2},
- the non diagonal components of [ϵ] are coupling coefficients:
  - the symmetric part [ϵ_S] of the coupling matrix corresponds to defects of parallelism or perpendicularity of the faces of the cubic proof mass: they are expected to be less than 10^{-5} rad,
  - the antisymmetric part [ϵ_{AS}] of the coupling matrix corresponds to misorientations, less than 10^{-3} rad, of the proof mass with respect to the gradiometer axes.

If the gradiometer is rigidly fixed in a non drag free satellite, the variations of the parasitic accelerations due to the drag and to the angular motion can reach 10^{-7} ms^{-2} in the measurement bandwidth. Thus, in this case, the necessary rejection ratio of these disturbances is 10^{-5} and that leads to match the scale factors and to correct the alignments of the accelerometers with the corresponding accuracies (i.e. for instance 10^{-5} for scale factors and 10^{-5} rad for axis alignments). An on board calibrating system and corrections via an on ground processing are necessary.

A calibrating system composed of three pairs of unbalanced wheels rotating at constant angular velocities ω_x, ω_y, ω_z has been proposed to that purpose [10]. The Figure 10 presents the configuration of these wheels around the centre of the eight three-axis accelerometers of the instrument.

Each pair of wheels apply to all accelerometers a sine wave calibrating acceleration. For instance, the acceleration provided by the wheels of axis $\vec{x}$ is:

$$\vec{\Gamma}_x = 2 \frac{\delta m}{M_S} l \, \omega_x^2 \begin{bmatrix} 0 \\ \cos \omega_x t \\ \sin \omega_x t \end{bmatrix}$$

where δm is the unbalanced mass of a wheel, l is its distance from the axis of the wheel.

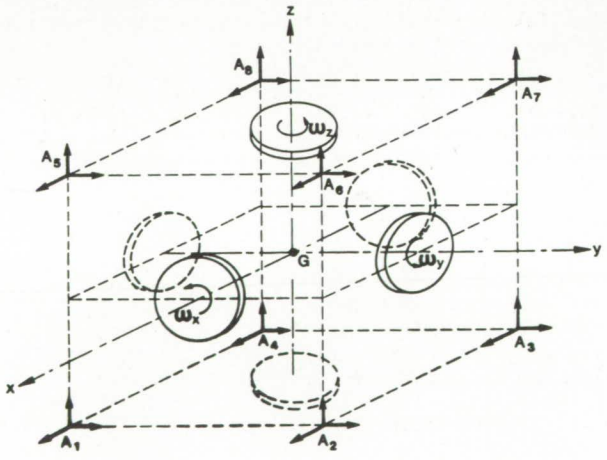

Fig. 10. On board calibrating system.

The measurement of Γ_x provided by an accelerometer is:

$$\vec{\Gamma}_x = 2 \frac{\delta m}{M_S} l \, \omega_x^2 \begin{bmatrix} \epsilon_x^y \cos \omega_x t + \epsilon_x^z \sin w_x t \\ (1 + \epsilon_y) \cos \omega_x t + \epsilon_y^z \sin \omega_x t \\ (1 + \epsilon_z) \sin \omega_x t + \epsilon_z^y \cos \omega_x t \end{bmatrix}$$

Synchronous demodulations at ω_x determine the following components:

- on axis $\vec{x}$:
  - in phase (cos): ϵ_x^y,
  - in quadrature (sin): ϵ_x^z;
- on axis $\vec{y}$, in phase (cos): $(1 + \epsilon_y)$;
- on axis $\vec{z}$, in quadrature (sin): $(1 + \epsilon_z)$.

These results are used for:

- in the one hand, the alignment of the axis $\vec{x}$ of the accelerometer,
- in the other hand, the matching of the scale factors of the two other axes.

In the same way, demodulations at angular frequencies ω_y and ω_z provide the necessary information to complete the alignment and the scale factor matching of all the axes.

A detailed analysis of the operation with an actual calibrating system has been performed [11].

6 - CONCLUSION

Presently most defined goals in geophysics, oceanography and geodesy, which are based on an improvement of the gravity field knowledge in the resolution range 100-200 km, can be reached in the near future by mapping the geopotential by means of a full tensor gradiometer on board a spacecraft orbiting the Earth on a quasi-polar, circular orbit at about 200 km altitude.

The gradiometer, based on differential accelerometry, consists of 8 three-axis electrostatic accelerometers located at the corners of a cubic structure with sides of half a meter.

The electrostatic accelerometers are designed to undergo accelerations of 10^{-4} ms^{-2} while providing a resolution better than 10^{-11} $ms^{-2}/\sqrt{Hz}$.

A dedicated satellite is necessary for the accomodation of this instrument. Two possible designs are considered for further developments:

- the GRADIO satellite, studied by the French Space Agency [11];
- the "Two-Stage Discos" configuration of the drag free satellite of the Geopotential Research Mission, studied by NASA [12].

7 - REFERENCES

[1] Balmino, G., Bernard, A., Satellite Gradiometry. Proceedings of the ESA Special Workshop SESAME, Ising am Chiemsee, March 4-6, 1986.

[2] Balmino, G., Letoquart, D., Barlier, F., Ducasse, M., Bernard, A., Sacleux, B., Bouzat, C., Runavot, J.J., Le Pichon, X., Souriau, M., Le projet GRADIO et la détermination à haute résolution du géopotentiel, Bull. Géod., 58, pp. 151-179, 1984.

[3] Kahn, W.D., Von Bun, F.O., Error analyses for a gravity gradiometer mission, IEEE Trans. on Geosc. and Rem. Sens., GE-23, n° 4, 1985.

[4] Rummel, R., Colombo, O.L., Gravity field determination from satellite gradiometry, Bull. Géod., 59, pp. 233-246, 1985.

[5] Bernard, A., Gay, M., Juillerat, R., The accelerometer CACTUS, AGARDograph n° 254, Avril 1982, "Advances in inertial systems and components".

[6] Boudon, Y., Bernard, A., Barlier, F., Juillerat, R., Mainguy, A.M., Walch, J.J., Synthèse des résultats en vol de l'accéléromètre CACTUS pour des accélérations inférieures à 10^{-9} G, 29ème Congrès IAF, Dubrovnik, 1978, publié dans Acta Astronautica.

[7] Bernard, A., Gay, M., Mainguy, A.M., SUPERCACTUS : projet d'accéléromètre triaxial à 10^{-11} G, 30ème Congrès IAF, Munich, 1979. Tiré-à-Part ONERA n° 1979-124, Acta Astronautica, 7, pp. 401-416.

[8] Mainguy, A.M., Bernard, A., Romero, M., Bouttes, J., Barlier,F., BIRAMIS : mesure du bilan radiatif de la Terre par microaccélérométrie spatiale. Congrès de la Société française de Physique, Toulouse, Juin 1979, Tiré-à-Part ONERA n° 1979-91.

[9] Bernard, A., Foulon, B., Le Clerc, G.M., Three-axis electrostatic accelerometer. Symp. Gyro Technology, Stuttgart, 1985.

[10] Bernard, A., Sacleux, B., Touboul, P., GRADIO: orbital gravity gradiometry through differential microaccelerometry, 34th International Astronautical Congress, Budapest, 9-15 octobre 1983. Publié dans Acta Astronautica.

[11] Balmino G. and al., Phase A: final report for a satellite gravity gradiometer experiment for the Geosciences, Rapport CNES, Janvier 1987.

[12] Touboul, P., Gradiometer accomodation on board a drag-free satellite, Matera, 29-30 avril 1987.

GRADIOMETER ACCOMMODATION ON BOARD A DRAG-FREE SATELLITE

P Touboul

ONERA, Châtillon, F

ABSTRACT

Satellite to Satellite Tracking (SST) and Satellite Gravity Gradiometry (SGG) are the two outstanding techniques for the global recovery of the Earth gravity field with a high resolution.

For both techniques, such a mission requires a dedicated satellite at a low altitude with fine orbit and attitude controls.

The brief studies, undertaken to investigate the accommodation of the GRADIO instrument (gradiometer developed in ONERA, France) on board one of the two spacecrafts of the Geopotential Research Mission (GRM) show that by taking advantage of the instrument resolution and of the spacecraft design, a very promising concept can be established.

A resolution of 10^{-2} Eötvös is then expected at an altitude of about 160 km.

1 - INTRODUCTION

The GRADIO instrument consists of eight three axis ultra-sensitive accelerometers located at the corners of a 0.5 m side cube. The electrostatic accelerometers have to undergo accelerations as large as a few 10^{-5} ms^{-2} and are designed in order to obtain a good linearity, a low coupling between the three axes and a resolution better than 10^{-11} $ms^{-2}/\sqrt{Hz}$ [1].

In the GRADIO mission, proposed to the European Space Agency [2,3], the instrument is rigidly fixed on board a dedicated satellite, and an original on board calibrating device is necessary to achieve the alignment, the scale factor matching, and the determination of the relative positions of the accelerometers.

With this gradiometer design and considering that the external forces and torques applied on it can be rejected with a 100 dB ratio, a resolution of better than 10^{-2} Eötvös/$\sqrt{Hz}$ is anticipated at an altitude of about 230 km.

A second option for the instrument accommodation has been investigated in ONERA in conjunction with NASA and APL*. The gradiometer is mounted on board one of the two drag-free satellites of the Geopotential Research Mission [4].

2 - TWO SPACECRAFTS FOR ONE INSTRUMENT

The GRADIO spacecraft configuration presented in Figure 1 and proposed by CNES is characterized by:

- an external spherical shape to minimize the atmospheric drag effects and the disturbing torques,
- a coïncidence between the satellite centre of mass, the gradiometer centre and the aerodynamic thrust centre (initial centring better than 5 mm),
- a conventional technology and a compatibility with Ariane IV dual launch in order to minimize the cost of the mission.

At the beginning of the mission the mass of the spacecraft is 1500 kg. The trade off between power supply and stabilization system performances leads to the choice of a 230 km synchronous orbit with 18 h ascending node local time. The six months mission is sufficient to obtain a global coverage of the Earth with a 50 km inter-track network.

The maximum atmospheric drag acceleration is lower than 10^{-4} ms^{-2}, full scale range of the accelerometers. The specific attitude control of the spacecraft leads to an Earth pointing stability better than 10^{-6} rad/s and 10^{-7} rad/s^{-2}, in term of angular velocity variations and angular acceleration variations.

The GRM mission consists of two drag-free satellites at an altitude of 160 km with a separation of 150 to 550 km. To obtain the gravity field, the relative velocity between the two satellites is measured and the gravity potential computed. The polar orbit is quasi circular and the propulsion system is designed to maintain the low orbit during six months.

*Applied Physics Laboratory

Proceedings of an ESA-NASA Workshop on a Joint Solid Earth Programme, Matera, Italy, 29-30 April, 1987 (ESA SP-1094, October 1987).

The spacecrafts shown in Figure 2, have a mass of about 2500 kg with 1400 kg of hydrazine fuel.

The maximum acceleration of the spacecraft are those provided by the thrusters to conteract the atmospheric drag force in all directions and to keep the reference mass centered. Along the track direction these accelerations can reach 7.5×10^{-4} ms^{-2}.

The accuracy of the present attitude control is of the order of 0.1° in a bandwidth of 0.2 rad/s. That leads to possible variations less than 2.10^{-4} rad/s and 10^{-5} rad/s^2 for the angular velocity and the angular acceleration.

The GRADIO spacecraft and the GRM spacecraft represent in fact the two possible designs for a gradiometry mission.

The drag-free satellite permits us to lower the altitude while keeping a very low level of accelerations applied to the instrument.

The GRADIO spacecraft is designed to minimize the angular accelerations of the spacecraft and then of the rigidly fixed instrument.

So the gradiometer accommodations are rather different. In the drag-free satellite, the gradiometer has to be fixed on a suspended stage which supports also the drag-free sensor, in order to be decoupled from the spacecraft parasitic motions.

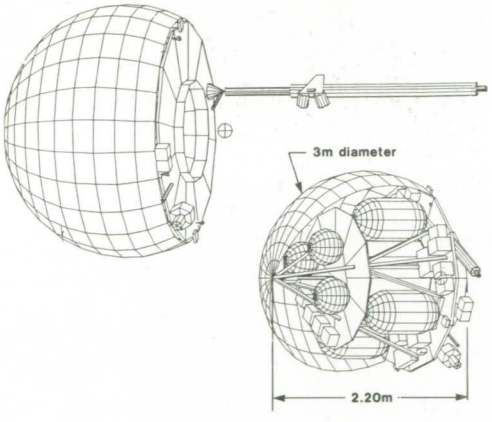

Fig. 1 - GRADIO Satellite.

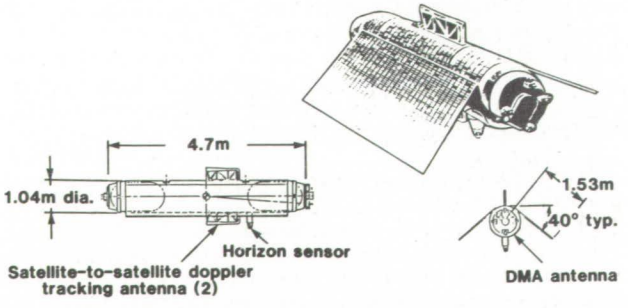

Fig. 2 - GRM drag-free satellite.

3 - GRADIO INSTRUMENT ACCOMMODATIONS ON BOARD A GRM SPACECRAFT

On board the drag-free GRM spacecraft the DISCOS sensor must be at the centre of mass in order to be not disturbed by the self gravity forces induced by the different parts of the spacecraft. At first sight, three possible configurations appeared to be considered for the gradiometer accommodation.

In the first case, the gradiometer is rigidly fixed on board the spacecraft but, is off-centered because of the DISCOS sensor location. The only advantage of this solution is the interface simplicity. But, the accelerometers have to sustain high levels of accelerations due to the drag compensation system, and then, have to be designed with a reduced sensitivity. Because the rejection ratio of the disturbing acceleration is limited by the accuracy of the scale factor matching (not fully achievable in this configuration) no gradiometry measurement are available during each firing.

With an off-centered gradiometer, the symmetry of the spacecraft cannot be maintained around the DISCOS and obviously around the gradiometer. The difficulties of the spacecraft design are increased and especially those relative to the changes in the spacecraft self-gravity.

All in all this solution appears to have no scientific interest.

In the second proposed configuration, the gradiometer is also off-centered but mounted on a suspended stage in order to lower the coupling between the instrument and the spacecraft motions, especially in the upper part of the instrument bandwidth. Even if the instrument calibration is made easier, this intermediate configuration, requires finally a difficult implementation for a low scientific interest.

The last and the only one attractive configuration assumes that the drag-free sensor is a two-stage DISCOS: the DISCOS sensor is fixed on a suspended structure to maintain the proof-mass of the sensor at the centre of its cage. Then the eight accelerometers of the gradiometer are fixed around the DISCOS on the same suspended inner-stage.

4 - TWO-STAGE DISCOS/GRADIO PRINCIPLE

The two-stage DISCOS/GRADIO accomodation is presently the most promising concept for the gradiometer integration on board a spacecraft.

The principles of this configuration are presented in Figure 3. The spacecraft is submitted to the external forces and torques, due to the atmospheric drag in particular, and to the thrusters. The spacecraft main-body is then moving in limit cycles around the magnetically suspended inner-stage. The magnetic suspension of the inner-stage is controlled to keep, on the one hand, the DISCOS proofmass at the center of its cage and, on the other hand, the inner-stage attitude Earth pointed. The eight three-axis accelerometers are symmetrically fixed around the DISCOS on the suspended intermediate stage. They provide the measurements of the linear and angular residual accelerations thus making it possible to improve the control of the magnetic suspension. Optical sensors are necessary to measure the position and the attitude of the inner-stage with respect to the spacecraft.

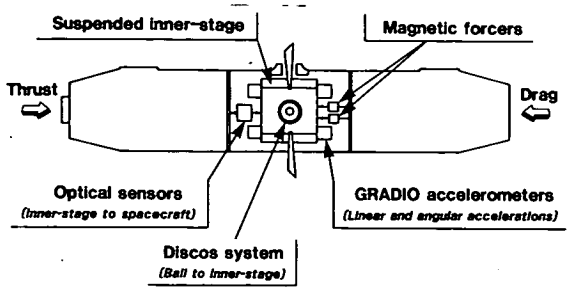

Fig. 3 - Two stage-DISCOS - GRADIO accommodation.

The main advantages of this concept are:

- the locations of the gradiometer and of the DISCOS sensor at the centre of the symmetrical distribution of mass corresponding to the spacecraft,
- the low level of residual accelerations applied to the instrument: in translation the inner-stage is drag-free according to the DISCOS measurements, and in rotation, the Earth pointed attitude is controlled through the GRADIO accelerometer measurements themselves,
- the low altitude of the spacecraft with a preserved high sensitivity of the accelerometers because the accelerations to undergo are, at least, not increased.

5 - INNER-STAGE CONTROL

The resolution for the gravity gradient measurements dramatically depends on the accuracy of the attitude and position controls of the inner-stage.

For each direction, the inner-stage position is controlled by means of two magnetic forcers acting in common mode in order to nullify the DISCOS capacitive sensor outputs (see Figure 4).

The angular acceleration of the inner-stage is controlled through the gradiometer measurements while the Earth pointed attitude is maintained through the optical sensors and the spacecraft attitude measurement system. For the two last controls, the forcers are acting in differential mode.

Because of the high resolution of the DISCOS sensor and its large bandwidth, the position control of the inner-stage does not seem to be the most critical point.

The inner-stage attitude control has to be carefully studied, because the required performances on the angular velocity and acceleration variations are stringent ($\Delta\Omega < 3.10^{-6}$ rads^{-2}; $\Delta\dot{\Omega} < 10^{-8}$ rads^{-2} in the measurement bandwidth), and because this control cannot be fully tested on ground.

The first analysis and simulations show that the angular control could be done for each axis according to the bloc-diagram presented in Figure 5.

The natural angular frequency of the inner-loop, used to control the angular acceleration, has to be as high as possible in order to minimize the effects of the disturbing torques acting on the inner-stage. An angular frequency of 10 rad/s is expected.

The natural angular frequency of the outer-loop necessary to keep the inner-stage attitude Earth pointed has to be low enough to filter out the angular motions of the spacecraft.

With the present characteristics of the attitude control of the spacecraft, this angular frequency would have be less than 10^{-3} rad/s to keep the angular acceleration variations less than 10^{-8} rad/s^2.

To make easier the inner-stage attitude control, the parasitic attitude motions of the spacecraft should be reduced by its aerodynamic design or by its attitude control system.

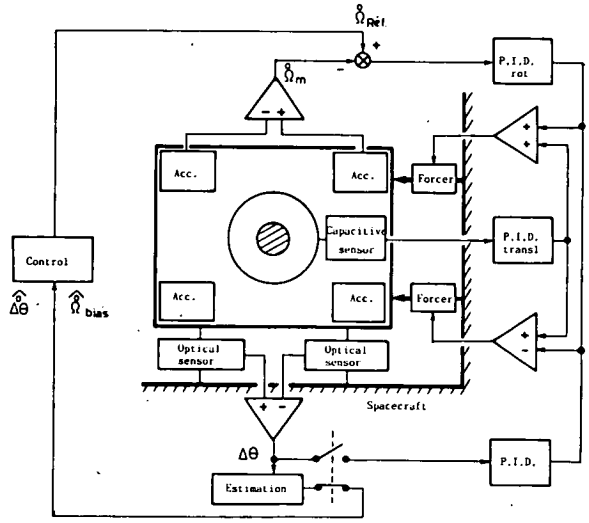

Fig. 4 - Inner-stage controls.

6 - EFFECTS OF CHANGE IN MASS DISTRIBUTION

Because of the relative motions of the inner-stage with respect to the spacecraft, one has to be very carefull of the mass distribution around the instrument.

However for a symmetrical distribution of mass, which is the base-line design of the configuration, the gravity gradient components at the centre of the distribution have only second order variations in all the directions.

The GRADIO configuration, with eight accelerometers at the corners of a centred cube, provides combinations of differential measurements, which precisely correspond to the gravity gradient at the center of the instrument, and thus of the mass distribution.

For instance, two symmetrical masses of 300 kg corresponding to the spacecraft structure, located at a distance of 1.15 m from the centre of the instrument induce variations of less than 5.10^{-2} Eötvös for relative displacements of 1 cm.

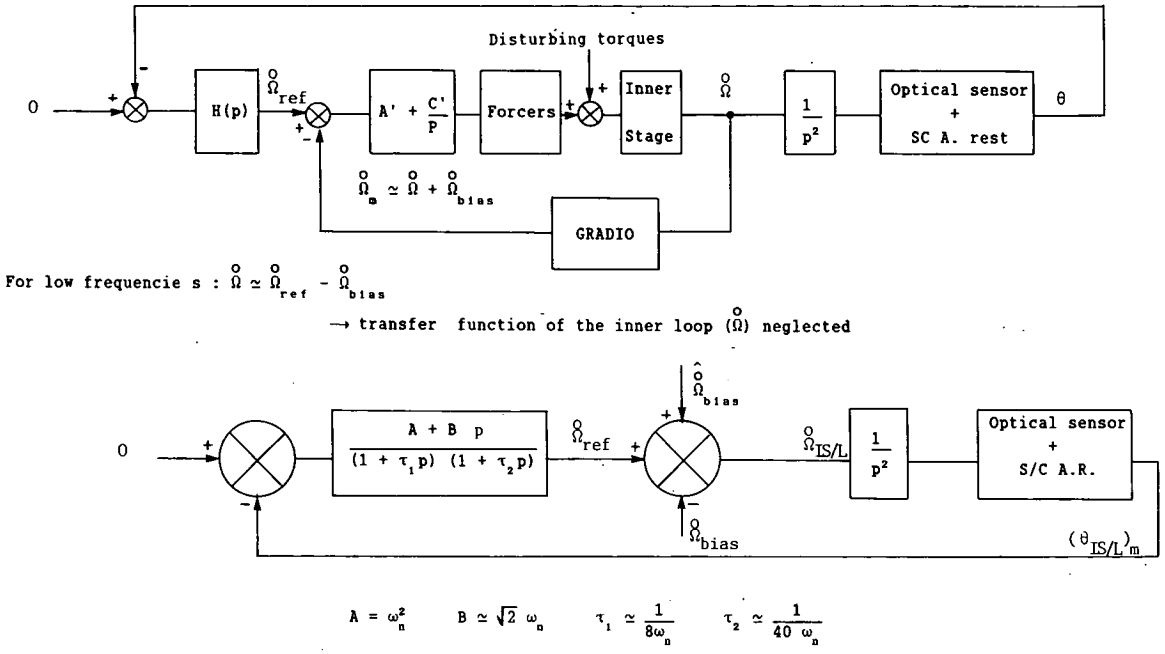

Fig. 5 - Attitude control of the inner-stage.

The measurements of the displacements provided by the optical sensors permits us to correct easily for such variations.

For a lack of symmetry, the effects depend dramatically on the distance between the accelerometers and the delta mass δM. Variations of 10^{-2} Eötvös correspond for instance to a displacement of 1 cm and to a δM of 5 kg at a distance of 1 m. Then it is necessary to maintain a sufficient distance between the accelerometers and the spacecraft elements which might not be exactly symmetrical.

7 - EFFECTS OF VIBRATION

The inner-stage is a quite complex structure which supports all the fine instrumentation, and might in particular carries the positionning antennas, or the Satellite-Satellite Tracking link antennas that are submitted to the atmospheric drag.

The deformation of the structure connecting the accelerometers, which is submitted to external excitations, can induce variations of the orientations of the accelerometer sensitive axes at the frequency of the external vibrations [5]. That can lead to rectification to these external vibrations producing a false gradient output (see Figure 6).

In the GRADIO three-axis accelerometers, the proof mass is electrostatically suspended in the three directions. The sensitive axes of these accelerometers are defined by the directions perpendicular to the cubic proof-mass faces. As the bandwidth of the attitude and position control servo-loops are limited to several hertz, the proof-mass does not follow the attitude and the position variations of the electrode sets fixed to the excitated structure. Thus, the rectification effects are dramatically filtered out when the modes of the structure are at a very higher frequency than the electrostatic suspension bandwidth.

This brings to light another interest in the use of three-axis accelerometers.

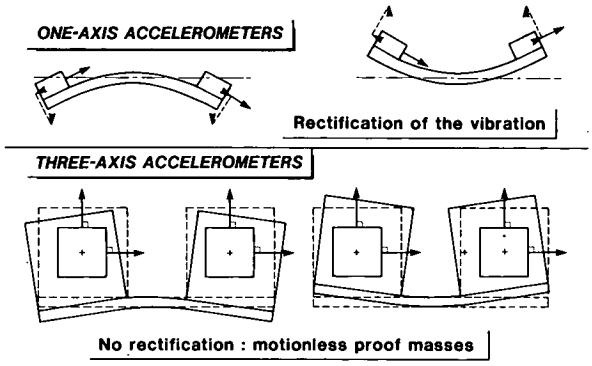

Fig. 6 - Effects of vibration.

NASA-ESA JOINT SOLID EARTH MISSION

GRADIO/TWO STAGE DISCOS GRM ACCOMODATION

ACTION ITEMS

1 - Attitude	*	*10 - Sensors performances*
2 - Error budget		*11 - Impact on GRM resources*
3 - Lab. models/tests	*	*11 - a. POWER*
4 - Data processing		*b. MASS*
5 - Self -calibration		*c. Data rate*
6 - Calibr. Wheels		*d. GRADIO configuration*
7 - Change-in-mass effects	*	*e. On board processing*
8 - Magnetic Fields effects		*f. Ground data handling*
9 - Failure mode analysis		*g. Operation Control*
		h. Thermal
		12 - Effect of vibration
		13 - Back-up mode

Table 1 - Gradio/Two stage Discos GRM accommodation: Action items.

8 - CONCLUSION

The GRADIO instrument is composed of eight three axis ultrasensitive accelerometers located at the corners of a cubic structure and requires for its accomodation on board a GRM spacecraft:

- a two-stage DISCOS configuration with a magnetically suspended inner-stage,

- a very fine control of the Earth pointed inner-stage taking into account the GRADIO accelerometer measurements in order to limit the variations of the angular accelerations.

Considering the results of all the action items that we have briefly undertaken in order to investigate the feasibility of such a mission (see Table 1) [6], for diagonal tensor components and an averaging time of 4 s, the present overall goal is 10^{-2} Eötvös at the altitude of 160 km.

REFERENCES

[1]. A. Bernard, GRADIO three-axis electrostatic accelerometers, Matera, 29-30 April 1987.

[2]. Balmino, G., Barlier, F., Bernard, A., Bouzat, C., Rummel, R., Touboul, P., Proposal for a satellite gravity gradiometer experiments for the geosciences

[3]. Balmino, F., Barlier, F., Bernard, A., Bouzat, C., Boullet, B., Pouzet, A.M., Rapp, E., Dufour, J., Rummel, R., Touboul, P., Phase A: final report for a satellite gravity gradiometer: experiment for the geosciences, January 1987.

[4]. T. Keating, P. Taylor, W. Kalin, F. Lerch, Geopotential Research Mission. Science, Engineering and Program Summary, NASA Technical Memorandum 86-240, May 1986.

[5]. D. Sonnabend, Vibration and differencing gravity gradiometers, Engineering Memo 314-388, October 1986.

[6]. A. Bernard, P. Touboul, Investigation for a joint mission GRADIO/GRM, Final Report ONERA n° 12/6114 PY, March 1987.

GRADIOMETER MISSION SPECTRAL ANALYSIS AND SIMULATION STUDIES PAST AND FUTURE

G Balmino

Bureau Gravimétrique International, Toulouse, F

ABSTRACT

This is a short review of past sensitivity analysis and simulation studies performed for a satellite gravity gradiometer (SGG) mission, and some ideas about necessary future numerical simulations.

1. INTRODUCTION

Gradiometry on board artificial satellites is a rather old concept, and a wealth, if not too many statistical analysis of the required sensitivity at given altitude and of the accuracy of the recovered functionals of the geopotential (gravity anomaly, geoid height) exist, but results are sometimes quite in disagreement. Only few numerical simulations have been made, which are promising steps towards the future more accurate simulations which must be performed in order to better understand the impact of instrumental errors on the computed quantities, and towards the real data processing methods themselves.

2. PAST SPECTRAL ANALYSIS STUDIES

These are analytical approaches based on the response of an instrument with given statistical characteristics (noise, sampling frequency, orbital coverage,...) to the excitation by a gravity field of assumed power spectra. The method may yield information on the r.m.s. error on recovered geodetic quantities. Table 1 lists some of the works performed in this direction in the last twenty years.

Table 1
Examples of SGG studies by the statistical approach

Author	Year	Findings[1]
Kaula	1968,1970	A
Lambeck	1974	A
Balmino et al.	1974,1984	A,C
Rummel	1979	A,B
Jekeli	1985	A,B
Kahn, Von Bun	1985	A,B
Robbins	1985	A,B

A : Resolution vs. gradiometer accuracy & altitude
B : Uncertainties of derived geodetic quantities
C : System error study

Few numerical simulations have been undertaken so far. The most important known ones are given in table 2. Their main feature is that geodetic quantities at the Earth surface are recovered as well as the uncertainties ; local studies only have been made - except the Rummel and Colombo simulation.

Table 2. Known numerical simulations in SGG

Author	Year	Method
Forward	1973	Point mass model & least squares
Reed	1973	Inversion of Stokes-Pizzetti operator by least squares
Ananda & Flury	1978	Point mass model & least squares - covariance analysis
Rummel & Colombo	1985	Zonal field and orbit recovery
Kahn	1986	Stokes-Pizzetti + a priori & orbital errors - covariance analysis
Bose	1983,87	Plane approximation, Karhunen-Loewe transformation
Ilk	1987	Stokes-Pizzetti + Tikhonov regularization

All authors have tried to solve an improperly posed problem, namely the local inversion and downward continuation of an integral equation from limited data outsides the Earth.

Results therefore very much depend on the a priori assumptions which are (and have to be) made and on the type of regularizing technique. Quoted uncertainties on geoid heights, or more commonly on $1^\circ \times 1^\circ$ (sometimes $0.5^\circ \times 0.5^\circ$) mean free air gravity anomalies recovered at the Earth surface, may vary by a factor of five from one author to the other.

Then the choice is clearly :

- either, and especially for geophysical applications of gradiometer data, to use the signal directly at satellite altitude,
- or to perform a full inversion by deriving a global gravity model, for instance in spherical

Proceedings of an ESA-NASA Workshop on a Joint Solid Earth Programme, Matera, Italy, 29-30 April, 1987 (ESA SP-1094, October 1987).

harmonics. This is a difficult and computer time consuming problem (considering the envisaged resolution of such model) and simulation studies must be conducted to assess and solve the critical points.

3. FUTURE SIMULATIONS TO BE DONE

The list of the simulation characteristics given below is certainly not exhaustive. Its purpose is to serve as a start for organizing the efforts to perform the necessary analysis.

The overall scheme of such simulations is represented on fig. 1. The framework is the usual one for orbit generation, determination (differential correction procedure) and is summarized in table 3.

Error models on the orbit could also be introduced by defining their spectrum with given amplitudes for each orbital parameter. The spacecraft attitude must also be modelized and a spectrum of errors on the Euler angles (or equivalent quaternion) be introduced.

One of the most important part in the simulation is a realistic (and obviously complicated) gradiometer error model to represent :

- the alignement and scale factor matching errors
- the biases
- the noise

Satellite disturbing effects (e.g. moving parts) must also be introduced.

Then two types of studies can be undertaken :

- again a series of local inversion with some type of regularization.

- a full recovery of the true spherical harmonics of the geopotential, probably together with the orbit and/or attitude parameters, along the lines of Rummel & Colombo, that is by a multistep iterative procedure.

CONCLUSION

It is urgent to undertake realistic full simulations of the GRADIO instrument and mission. Some points have been identified already but further analysis of the critical problems have yet to be made. Existing softwares available in european groups must be used as much as possible, although some parts will have to be modified or rewritten. Target computers must also be identified. The whole task must be viewed as a preparation to the real data reduction works of the future.

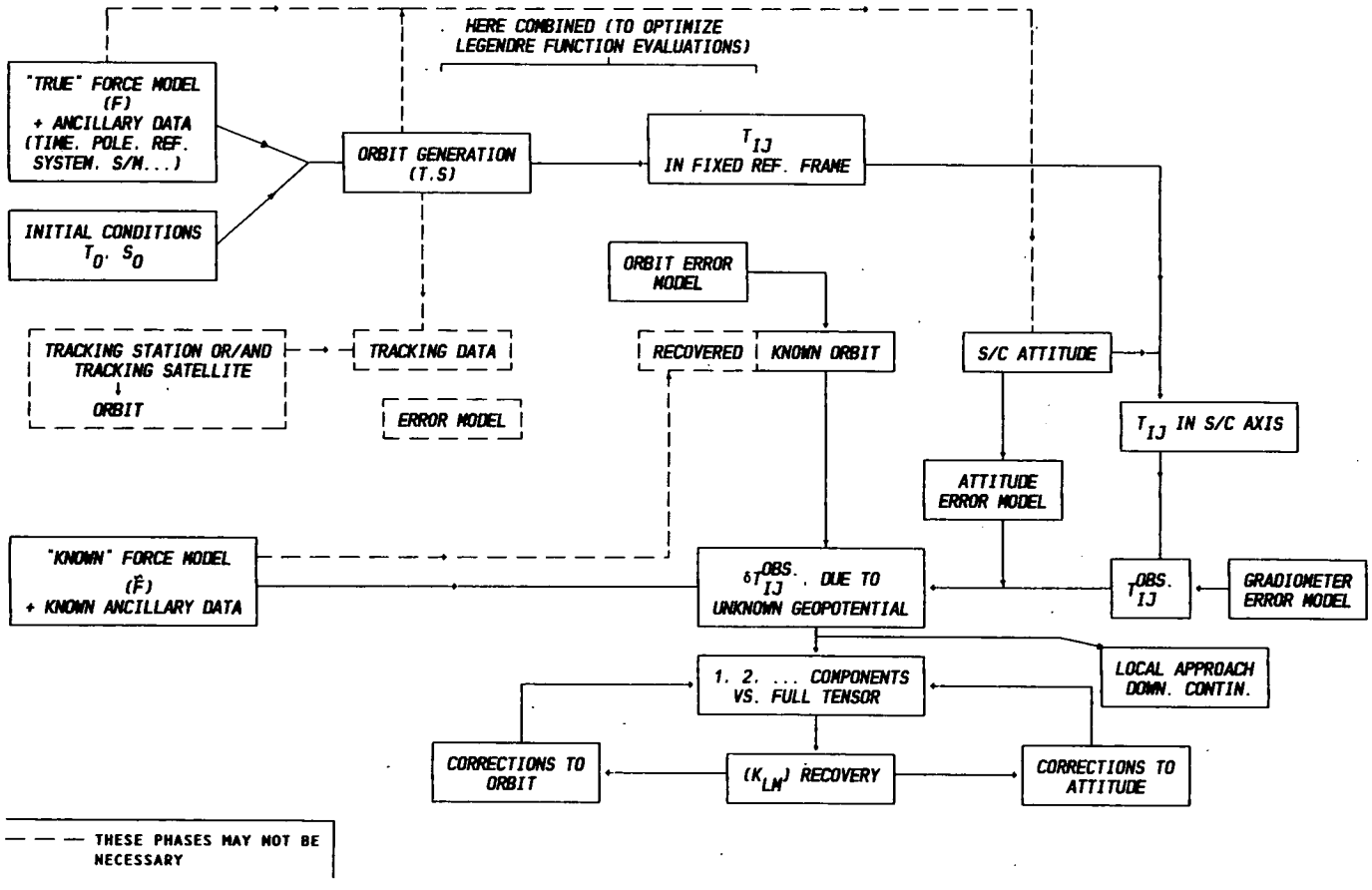

Figure 1: General scheme of an elaborate SGG simulation study.

Table 3. Simulation studies ; framework

Item	Characteristics
Time Scale	Solar barycentric time
Reference System	True celestial system - IAU 1980 Precession + Nutation + apparent accelerations / J 2000 mean celestial system. Pole, UT1 : from BIH
"True" force model	Earth geopotential : harmonics to degree and order L $180 \leq L \leq 360$ Luni-solar effects : . direct (DE200 JPL ephemeris) . tides : solid, oceanic (Merit standards) Surface forces : . Drag DTM model . Solar pressure: direct earth albedo
"Known" force model	Earth geopotential : e.g. GRIM 3L1 (to 36,36) Ocean tide model different from "true" one Non gravitational forces : Drag Jacchia 71 model Solar pressure : few % errors on parameters.
Orbit generation & computation of gravity tensor	Integrator : Cowell, regularized (+ Encke formulations) Stepsize : 5 to 10 sec. Legendre functions : Pine's formulation, vectorized Arc length : 1 month at least + orbital manoeuvers possible (→ restart...)

CONCEPT OF AN OPTO-ELECTRONIC ACCELEROMETER SYSTEM (OAS)

B Kunkel, K Keller & R Lutz

MBB, Space Systems Group, Ottobrunn, FRG

Summary

This paper essentially presents the progress compared to a previous paper given at the 1986 Ising SESAME Solid Earth Workshop.
A brief conceptual description of the OAS is given first. For a more detailed description we refer to the SESAME Proceedings. MBB has continued the elaboration of the Position Sensitive Detector (PSD) core unit of the OAS development on inhouse fundings. The achieved measurement results in terms of resolution of the motion of a gravity gradient sensitive reference mass exceed the before specified resolution requirement substantially such that a gravity gradient accuracy of $\leq 10^{-2}$ E.U. or $\leq 10^{-12}$ g would be feasible. Examples of relevant measurement results are presented.

1. Introduction

The concept of an accelerometer based on a spring-suspended reference mass and its precise relative motion measurement by means of 3 two-dimensional PSD's has been presented at the SESAME Workshop in March 1986.
This concept could be used in a set of 2-h OAS to form an extremely sensitive spaceborne gradiometer.
In view of the advancements of the ONERA "GRADIO" instruments, however, which has been reached the status of a complete prototype model, this concept apparently suffers from being proposed too late. However, it should be worthwhile to realise a complete OAS single accelerometer laboratory model in order to compare the performance under ground-based test conditions, and, to have a technical backup solution available in time.
Since the ESA Solid Earth Programme now is emphasizing a gradiometer mission with a 1993 launch date (dual launch with ERS-2), the finally presented development plan clearly shows that an OAS based gradiometer mission would meet such a launch date. As the OAS is based on components which inhere no technical risk for long-term spaceborne missions, the extension of the MBB development effort towards an alternative gradiometer concept is strongly recommended.

2. Brief Summary of Measurement Objectives

The improvement need of the geopotential gravity field determination is commonly agreed among the related scientific community.

Such improvement would have, besides the tectonics of the Earth's mantle and sub-mantle layers research, also practicable applications such as more precise orbit ephemerides calculations.
The starting point for the OAS conception was a gradiometer concept based on a flexible mechanical suspension of a proof mass, different from commonly used electrostatic or electromagnetic suspension of a reference mass. The motion of such a proof mass by excitation through acceleration forces such as geopotential gradients, atmospheric drag or solar wind pressure gradients was to be detected. Typically, laser interferometers have been proposed to measure such relative motion with a resolution in the order of 10^{-7} m (100 nm) in order to measure acceleration gradients of about 10^{-11} g.
Such relative motion resolution has been achieved at MBB one year ago with a relatively new and simple two-dimensional but single detector system, the "position sensitive detector" (PSD). Thus, it was a straight-forward concept to combine the measurement requirements and this kind of sensor which MBB has succeeded to improve to much higher geometric resolution than specified.

3. OAS Measurement Principle

The OAS concept has been presented at the Ising SESAME Workshop and in its Proceedings already. This, a rather brief description is repeated herewith.

The OAS principle is illustrated in a simplified sketch, see Fig. 1 with a 2-dimensional scheme: the proof mass is suspended by 4 soft springs compensation of larger perturbation forces, a piezo-controlled pretension is applied (for the launch survival, additional clamp mechanisms for the reference mass are foreseen).
The main OAS element is the Position Sensitive Detector (PSD), i.e. the opto-electronical motion measurement unit. The functional principle of this 2-dimensional dual layer PIN diode is schematically shown in Fig. 2.

Proceedings of an ESA-NASA Workshop on a Joint Solid Earth Programme, Matera, Italy, 29-30 April, 1987 (ESA SP-1094, October 1987).

Fig. 3 illustrates the 6 degrees of freedom measurement coordinate frame which is covered by one OAS unit. Two such OAS units would form, at a certain spatial separation off a satellite CoG, the simplest gradiometer. Due to the 6 DOF measurement capability per accelerometer, any additional OAS would represent a redundancy or calibration unit. The drawing also indicates the pretension control of the springs by piezo-transducers, thus providing an adjustable dynamic range. A further magnetic or inductive control force can be applied to limit the amplitude and oscillation of the proof mass. A first conception of the physical layout is shown in Fig. 4. Note that due to the very recent improvements of the reference mass motion measurement a significant reduction of the physical dimensions is a likely consequence.

A schematic block diagramme of the OAS electronics is shown in Fig. 5; it is based on a central preprocessing and processing electronics for all 3 PSD sensors per accelerometer or gradiometer. This together with the central (single) illumination source should ease the calibration problem.

4. OAS-Performance

Compared to the motion resolution of 100 nm as required in sect. 2 to measure a gravity gradient of $\leq 10^{-11}$ g, the second MBB breadboard revealed a resolution (longterm linearity) of about 25 nm in one direction (due to the physical principle of the PSD, the second layer is slightly less sensitive than the top layer; accordingly for the gravity gradient detection one would select the more sensitive layer for the Z/X component detection). This factor of 4 improvement can be increased to a factor of 20 easily by:

- using a thermo-electric cooler for temperature stabilisation of the PSD's (factor of 2 - 2.5)
- using an appropriate short distance/focal length optics; the currently used is optimised for > 0.3 m distance (factor of 4)

Consequently, a $\leq$ 10 nm motion resolution can be achieved at readout frequencies of 10 - 20 Hz, or 50 nm at $\leq$ 100 Hz. Thus, at 10 Hz sampling rate an acceleration gradient of $\leq 10^{-12}$ g (or the equivalent of $\leq 10^{-3}$E or $\leq 10^{-4}$ m Gal/km) would be detectable. (Fig. 6).

At this level, however, the OAS is believed to be at the reasonable limits though, theoretically, better resolution should be feasible. The practical limits will be imposed by the thermo-mechanical stability of the housing (defining the extension of the reference mass suspension length).

5. Development Plan

Since the optoelectronic or measurement part of the OAS has been verified in the laboratory and only the mechanical part has to specified and be verified (dimensions, reference mass, suspension, control forces) in a computer simulation, there is no apparent risk in a two-step development approach towards a spaceborne version. No space-critical items are applied, thus, there is no particular qualification procedure except for the launch clamp mechanism.
A typical development plan is outlined in Fig. 7, aiming at a launch readiness in mid 1992, provided, the development is initiated soon. Until now, only MBB inhouse funding has been used for the conception and breadboarding.
The development effort will depend on the model philosophy, but will remain rather moderate for the reasons given above.

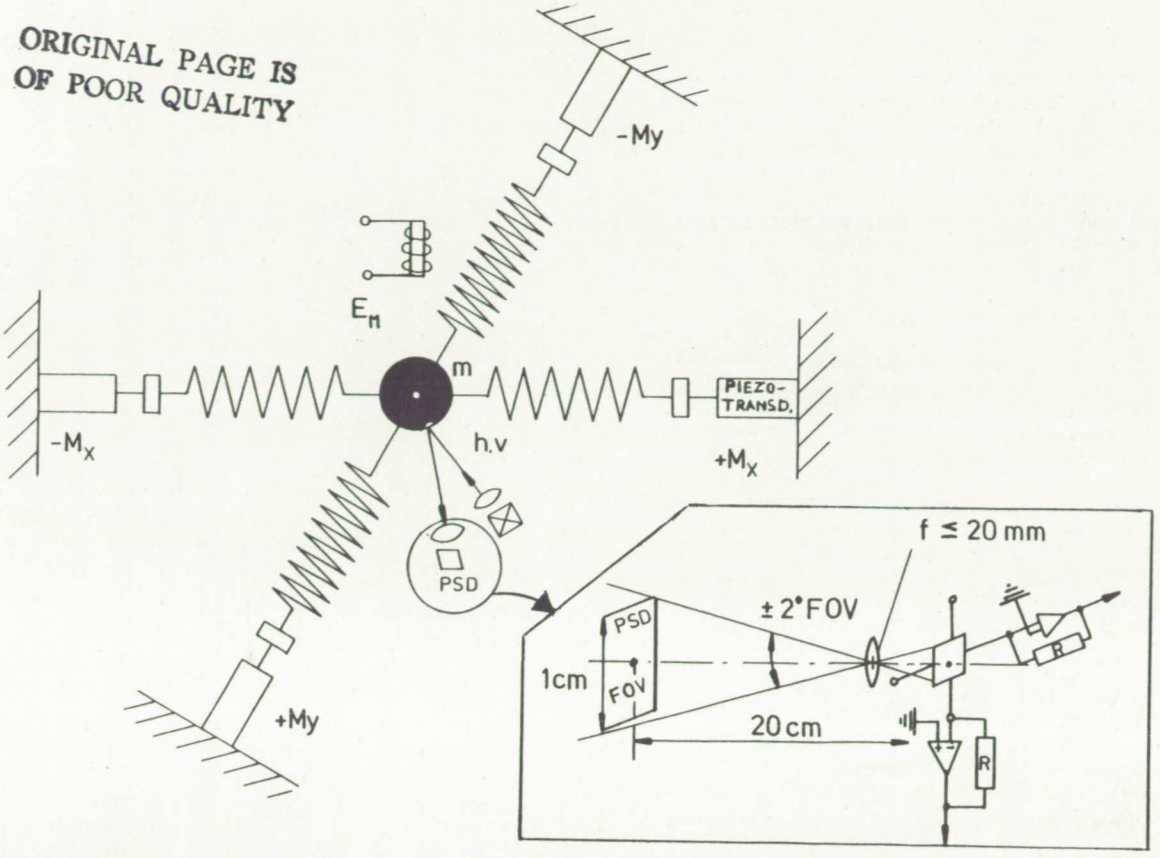

Fig. 1: OAS basic measurement principle
(1 observation plane only)

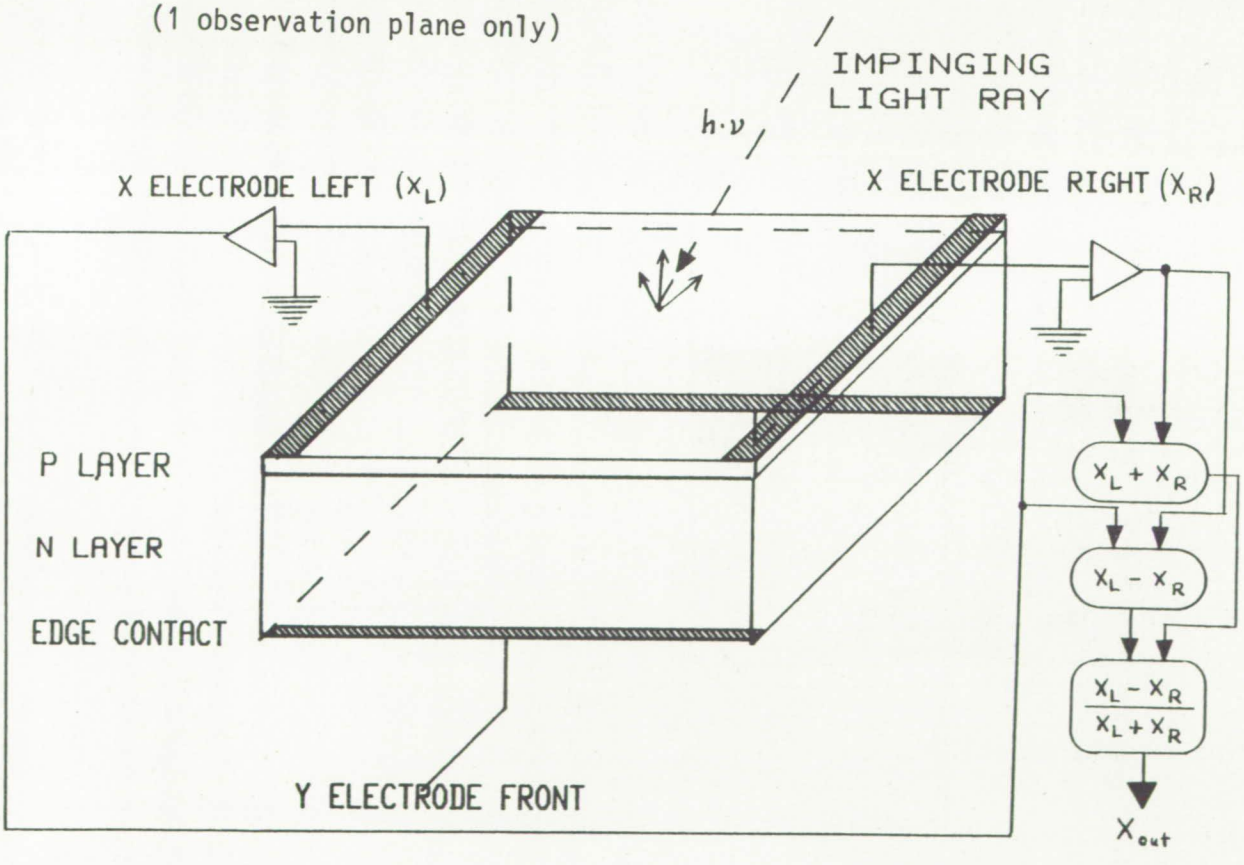

Fig. 2: PSD Functional Principle

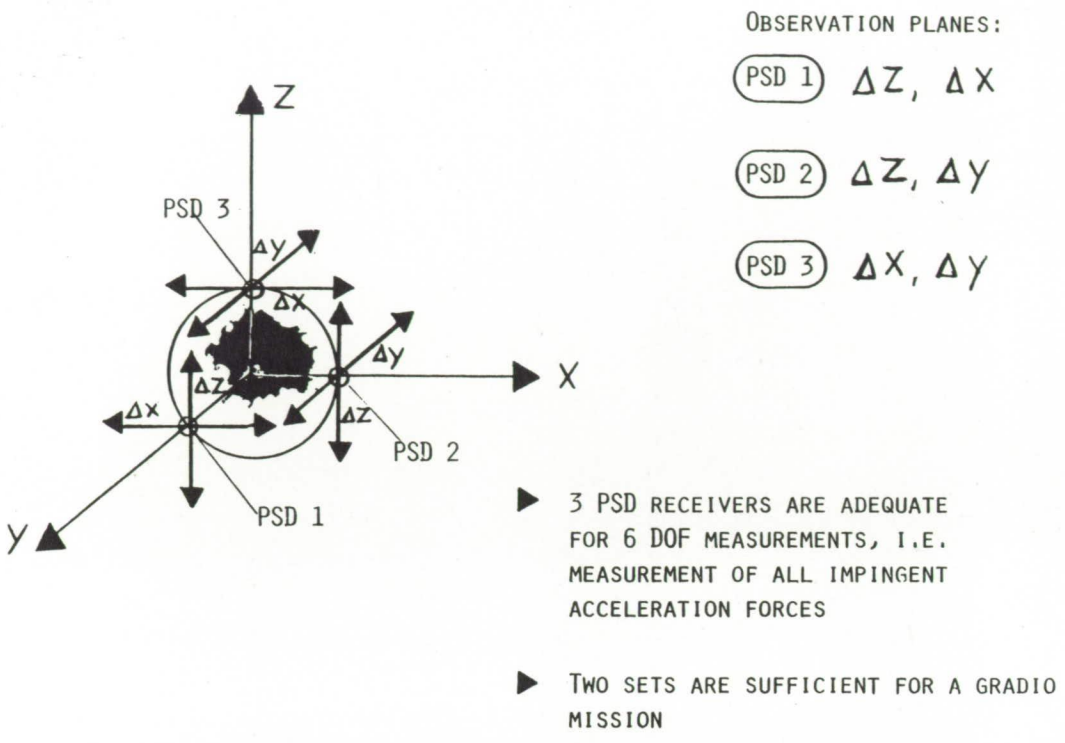

Fig. 3: OAS Measurement Coordinate System

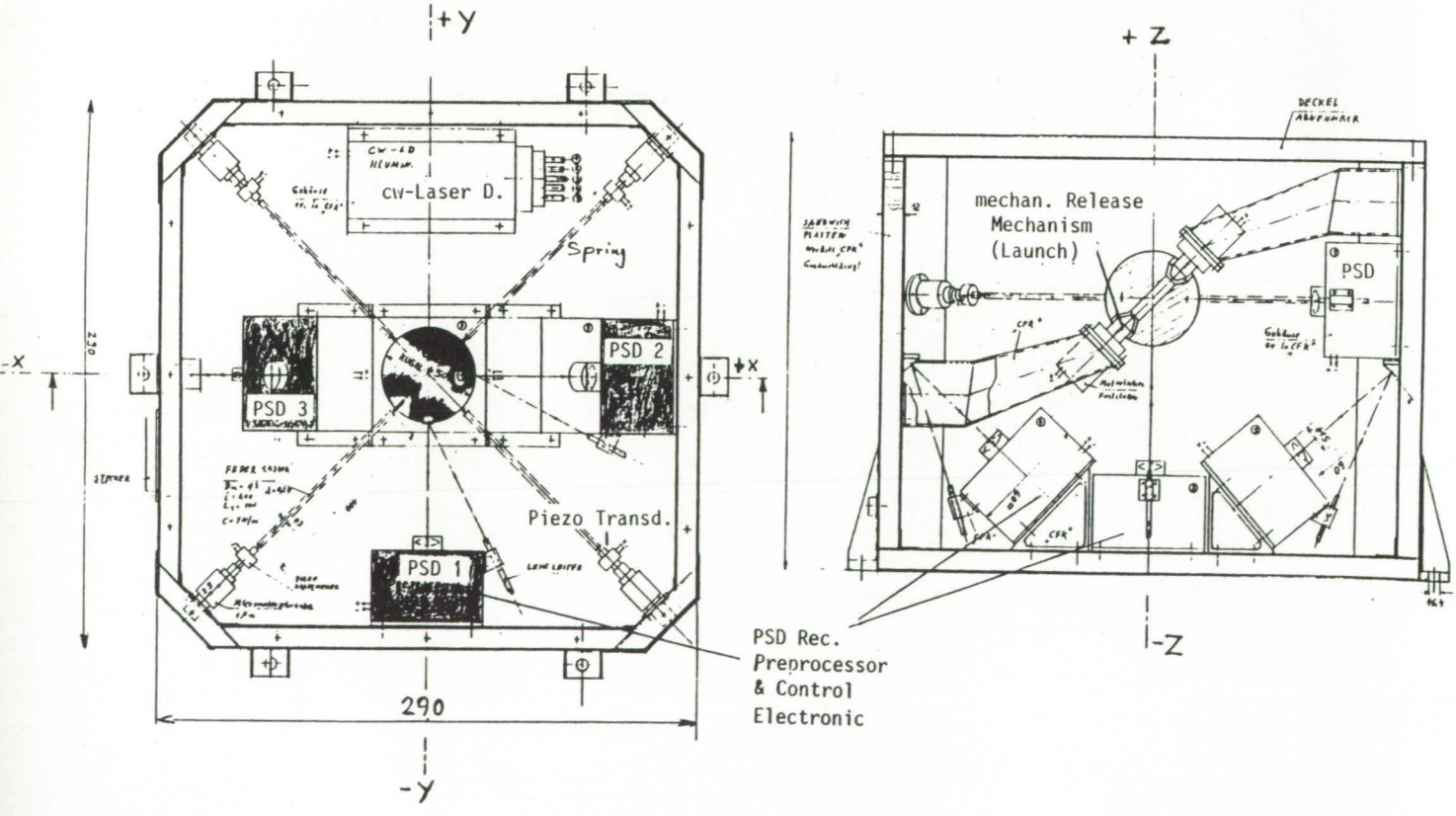

Fig. 4: Total OAS Accelerometer Setup, initial concept

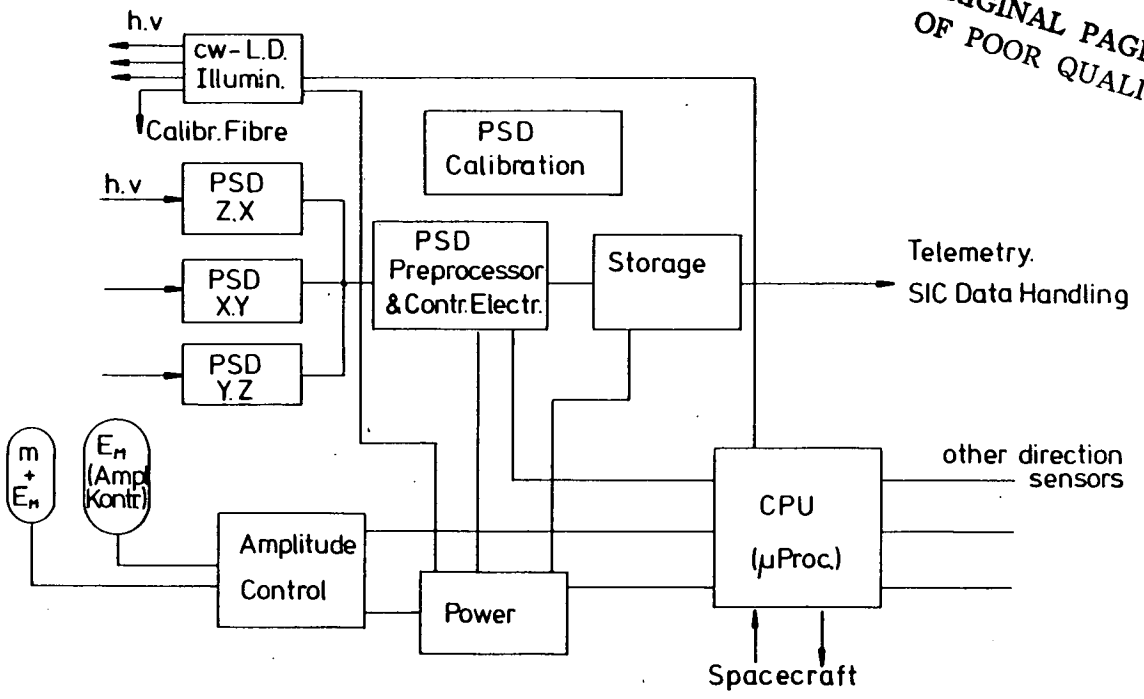

Fig. 5: Total OAS Electronics Block Diagramme

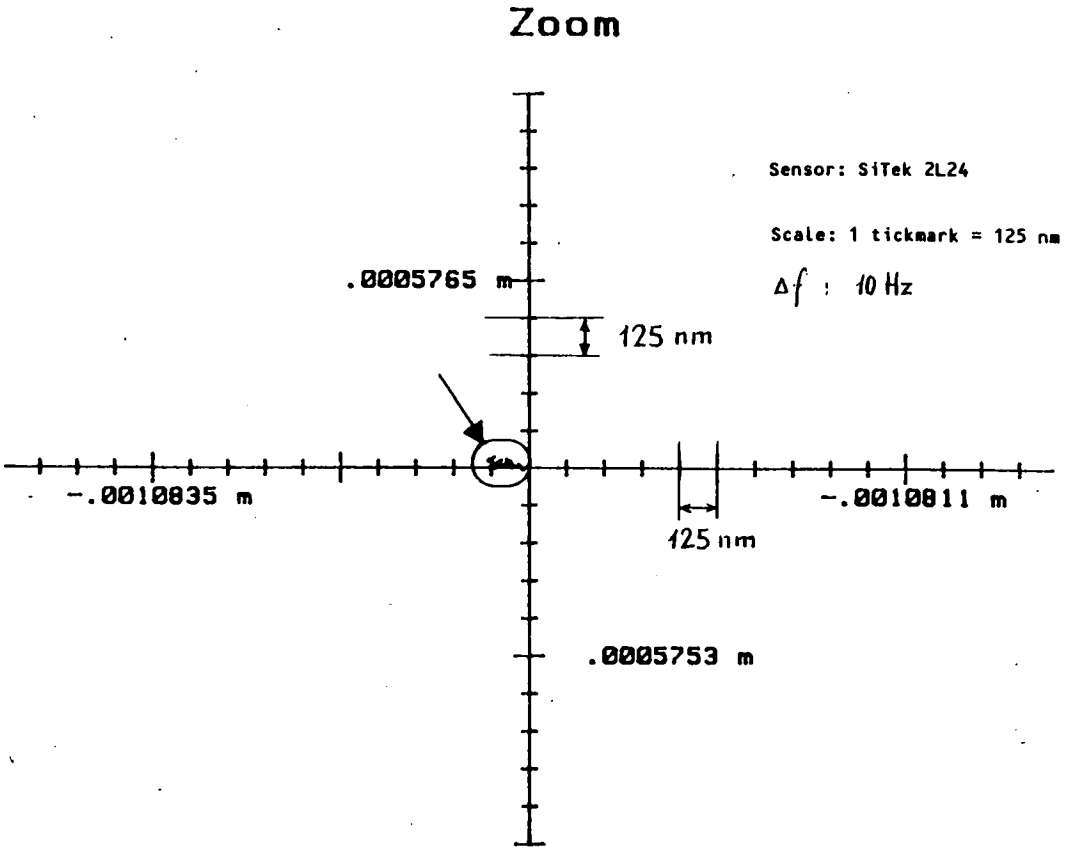

Fig. 6: MBB OAS/PSD Breadboard Performance Example

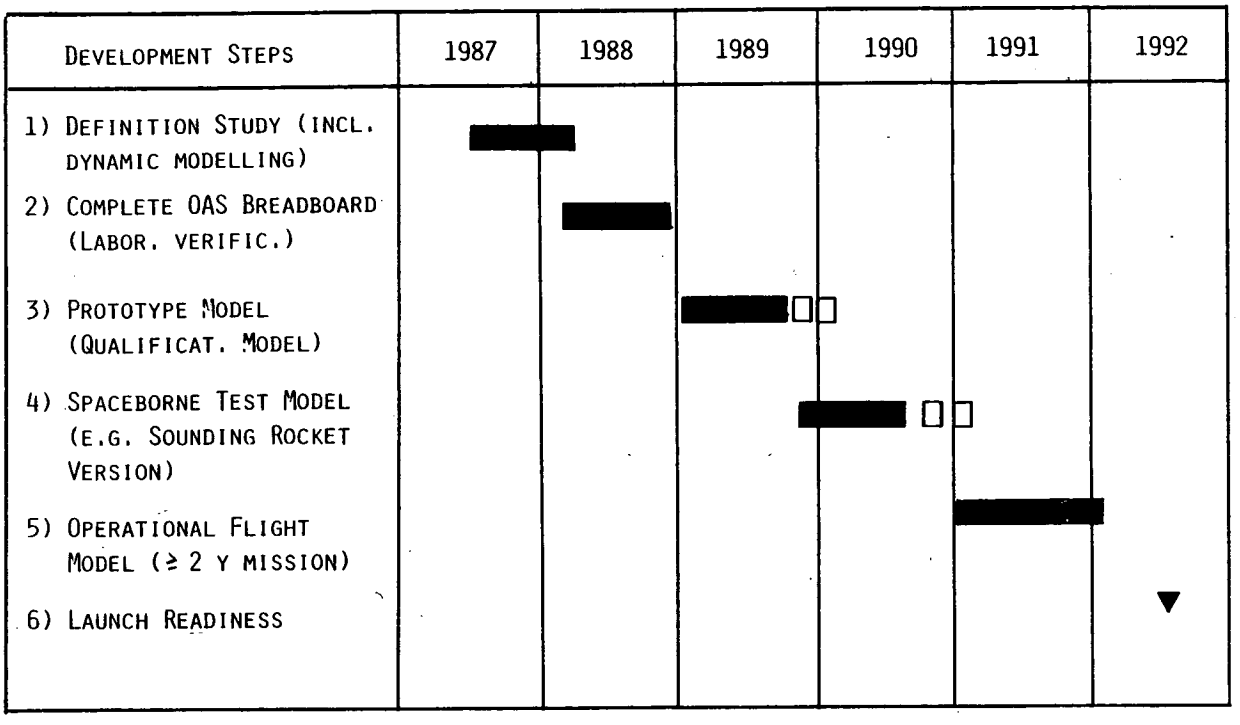

Fig. 7. OAS Development Plan (until operational spaceborne version)

List of Participants

FRANCE

Dr J. ACHACHE
Responsable de l'Equipe Magnetisme Spatial
Laboratoire de Géomagnétisme
Institut de Physique du Globe de Paris
4 Place Jussieu
75005 PARIS

Dr G. BALMINO
Directeur du Bureau Gravimétrique International
CNES/GRGS
18 Avenue E. Belin
31055 TOULOUSE Cedex

Dr A. BERNARD
ONERA
29 Av. de la Division Leclerc
(B.P. 72 - 92322 CHATILLON Cedex)

Mr P TOUBOUL -> see Bernard
ONERA

Dr S. COUTIN
Responsable des Programmes de Physique du Globe
CNES
Direction des Programmes
2 Place Maurice Quentin
75039 PARIS CEDEX 01

Dr C. ETIENNE
MATRA
Direction Technique Etudes et Ingénierie
31 rue des Cosmonautes
Z.I. du Palays
31077 TOULOUSE Cedex

Mr A PERALDI -> see Etienne
MATRA

Mr P EXERTIER
CERGA/GRGS
Avenue Copernic
06130 GRASSE

Mr R GUILLET
SAGEM
Centre d'Etudes ERAGNY
Av. des Gros Chêne
B.P. 51
95612 CERGY-PONTOISE Cedex

Mrs J RUNAVOT
CNES
18 Av. Edouard Belin
Batiment PMF
TOULOUSE

GERMANY

Dr R. BENZ
Dornier System, Dept. ERYT
Postfach 1360
D-7990 Friedrichshafen
ALLEMAGNE

Mr K. JÄGER
DFVLR
Linder Höhe
Postfach 906058
D-5000 KÖLN 90
ALLEMAGNE

Mr B. KUNKEL
MBB GmbH, Abt. RA 42
Postfach 80 11 69
8000 MÜNCHEN 80
ALLEMAGNE

Mr B SCHUERENBERG
Dornier System
Postfach 1360
7990 Friedrichshafen
ALLEMAGNE

Prof. Dr. C. REIGBER
Deutsches Geodätisches Forschungsinstitut
Marstallplatz 8
8000 München 22
ALLEMAGNE

Dr A. ROSSBACH
DFVLR Oberpfaffenhofen
D-8031 OBERPFAFFENHOFEN
Post Wessling
ALLEMAGNE

Prof. Dr J. ZSCHAU
Universität Kiel
Institut für Geophysik
Olshausenstr.
D-23 KIEL 1
ALLEMAGNE

Mr E GROTEN
Techn. Univ. Darmstadt
Institut f. Physik Geodäsie
Petersenstr.13
GI-DARMSTADT

NORWAY

Prof. K. AKSNES
Norwegian Defense Research Establishment
Box 25
2007 Kjeller
Norvege

BELGIUM

Prof. P. PAQUET
Observatoire Royal de Belgique
Avenue Circulaire, 3
1180 BRUXELLES
(Belgique)

UNITED KINGDOM

Dr R. HOLDAWAY
Satellites International Ltd
The Paddock; Hambridge Road
Newbury; BERKS RG14 5TQ
ANGLETERRE

Dr J.G. OLLIVER
Oxford University
Dept. of Earth Sciences
62 Banbury Road
OXFORD OX2 GPN

Dr. D.R. BARRACLOUGH
Geomagnetism Research Group
British Geological Survey
Murchison House
West Mains Road
EDINBBURGH EH9 3LA
ECOSSE

Mr Jack WEIGHTMAN
44 Aytoun Road
GLASGOW G41 5HN
ECOSSE

USA

P TAYLOR
NASA/GSFC
Gephysics Branch
CODE 622
Greenbelt, Maryland
20771 USA

H FOX
APL/JHU
Space Department
Johns Hopkins Road
LAUREL, Md
20707 USA

T KEATING
NASA/GSFC
CODE 402
Greenbelt, Md
20771 US

E A FLINN
NASA HQ
Acting Chief Geodynamics Branch
Office of Space Science & Applications
Washington DC
20546 USA

USA CONT.

D MCADOO
NASA HQ
Office of Space Science & Applications
Geodynamics Branch
Washington DC
20546 USA

W KAULA
NOAA
Director National Geodetic Survey
National Oceanic & Atmospheric Administratio
Rockville, Maryland
20852 USA

D SONNABEND
CALTECH/JPL
4800 Oak Grove Drive
PASADENA,
CAL. 91109 USA

Prof. R RAPP
OHIO STATE UNIV.
Dept. of Geodetic Science
1958 Neil Avenue
COLUMBUS, OHIO 4321o

ITALY

Dr BARRESI
Italspazio
Via V.E. Orlando 83
00185 ROMA
ITALIE

Dr B. BENCIOLINI
Ist. Topografica Fotogrammetria e Geofisica
Piazza L. Da Vinci-32
MILANO
ITALIE

Mr A. CAPORALI
Dipartimento di Fisica G. Galilei
Universita di Padova
Via Marzolo no. 3
I-35131 PADOVA
ITALIE

Prof. L. GUERRIERO
CNR
Piano Spaziale Nazionale
Viale Regina Margherita 202
00198 ROMA
ITALIE

Prof.S. LESCHIUTTA
Politecnico di Torino
Dipartimento di Elettronica
Corso Duca degli Abruzzi 24
10129 TORINO
ITALIE

ITALY CONT.

Dr G. SYLOS LABINY
CNR
Piano Spaziale Nazionale
Viale Regina Margherita 202
00198 ROMA

Dr A DALL'OGLIO
Ist. Nazionale di Geofisica
Dipartimento di Fisica
Viale Berti Pichat 8
40127 BOLOGNA

D GALIMBERTI
LABEN
Strada Padana Superiore 290
I-20090 VIMODRONE
MILANO

G VERRONE
Dip. di Fisica
Univ. di Bari
BARI

B PERNICE
Dip. di Fisica
Univ. di Bari
BARI

G BIANCO
PSN/CNR -> Via Sylos-Labini
MATERA

G VARESIO
AERITALIA
Settore Spazio
Corso Marche 41
I-10146 TORINO

Mrs A PRATA
PSN/CNR -> Via Sylos-Labini

I VARANNO
OFFICINE GALILEO
Via I Einstein 35
I-50013 CAMPI BISENZIO

G PERALDO
TELESPAZIO
Via Alberto Bergamini 50
I-000159 ROMA

F PALUTAN -> see Peraldo
TELESPAZIO

Mrs C ROSINI
PSN/CNR -> Via Sylos-Labini

I BARRACO -> see Varesio
AERITALIA

S CARRETTA -> see Peraldo
TELESPAZIO